HHS Public Access

Author manuscript

Cell Rep. Author manuscript; available in PMC 2023 October 23.

Published in final edited form as:

Cell Rep. 2023 April 25; 42(4): 112381. doi:10.1016/j.celrep.2023.112381.

FXR1 regulates vascular smooth muscle cell cytoskeleton, VSMC contractility, and blood pressure by multiple mechanisms

Amanda St. Paul[1], **Cali Corbett**[1], **Amanda Peluzzo**[1], **Sheri Kelemen**[1], **Rachael Okune**[1], **Dale S. Haines**[2], **Kyle Preston**[1], **Satoru Eguchi**[3], **Michael V. Autieri**[1,4,*]

[1]Lemole Center for Integrated Lymphatics Research, Lewis Katz School of Medicine at Temple University, Philadelphia, PA 19140, USA

[2]Department of Medical Genetics and Molecular Biochemistry, Lewis Katz School of Medicine at Temple University, Philadelphia, PA 19140, USA

[3]Cardiovascular Research Center, Lewis Katz School of Medicine at Temple University, Philadelphia, PA 19140, USA

[4]Lead contact

SUMMARY

Appropriate cytoskeletal organization is essential for vascular smooth muscle cell (VSMC) conditions such as hypertension. This study identifies FXR1 as a key protein linking cytoskeletal dynamics with mRNA stability. RNA immunoprecipitation sequencing (RIP-seq) in human VSMCs identifies that FXR1 binds to mRNA associated with cytoskeletal dynamics, and FXR1 depletion decreases their mRNA stability. FXR1 binds and regulates actin polymerization. Mass spectrometry identifies that FXR1 interacts with cytoskeletal proteins, particularly Arp2, a protein crucial for VSMC contraction, and CYFIP1, a WASP family verprolin-homologous protein (WAVE) regulatory complex (WRC) protein that links mRNA processing with actin polymerization. Depletion of FXR1 decreases the cytoskeletal processes of adhesion, migration, contraction, and GTPase activation. Using telemetry, conditional $FXR1^{SMC/SMC}$ mice have decreased blood pressure and an abundance of cytoskeletal-associated transcripts. This indicates that FXR1 is a muscle-enhanced WRC modulatory protein that regulates VSMC cytoskeletal

*Correspondence: mautieri@temple.edu.

AUTHOR CONTRIBUTIONS

A.S.P. performed the majority of the molecular biology, cell culture, and *ex vivo* experiments. A.S.P created the graphical abstract using BioRender.com. C.C. performed cell culture and *ex vivo* experiments. A.P. performed *ex vivo* experiments. S.K. and R.O. performed immunohistochemistry. D.S.H. interpreted and performed MS data. K.P. performed mouse telemetry. S.E. provided the $SmMHC\text{-}CreER^{T2}$ mouse and telemetry equipment. M.V.A. designed experiments, interpreted data, performed some western blots, and wrote the majority of the manuscript.

DECLARATION OF INTERESTS

The authors have no interests to disclose.

SUPPLEMENTAL INFORMATION

Supplemental information can be found online at https://doi.org/10.1016/j.celrep.2023.112381.

INCLUSION AND DIVERSITY

One or more of the authors of this paper self-identifies as an underrepresented ethnic minority in their field of research or within their geographical location. One or more of the authors of this paper self-identifies as a gender minority in their field of research. One or more of the authors of this paper received support from a program designed to increase minority representation in their field of research. We support inclusive, diverse, and equitable conduct of research.

dynamics by regulation of cytoskeletal mRNA stability and actin polymerization and cytoskeletal protein-protein interactions, which can regulate blood pressure.

In brief

St. Paul et al. show that FXR1 links mRNA processing with actin dynamics in vascular smooth muscle cells by binding to mRNAs and proteins that regulate the cytoskeleton. Deletion of FXR1 leads to decreased cellular migration, adhesion, and contraction. Additionally, mice without FXR1 have decreased blood pressure.

Graphical Abstract

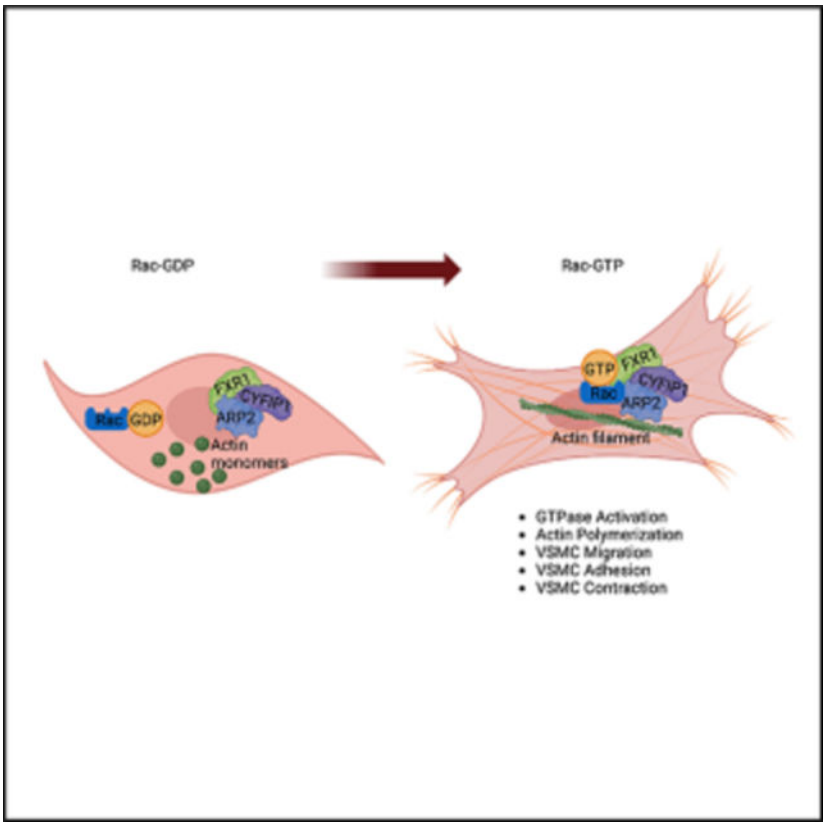

INTRODUCTION

Hypertension is a major risk factor for heart disease and stroke. Current treatments such as diuretics, angiotensin-converting enzymes (ACEs; ACE inhibitors), angiotensin II receptor blockers (ARBSs), and calcium channel blockers that act on blood vessels are not effective for all patients and have unfavorable off-target effects.[1] Even when optimally treated, hypertensive patients still have a 50% greater cardiovascular risk than untreated normotensive subjects, and effective treatments with minimal off-target effects are needed. A reevaluation of our understanding of the regulation of blood pressure with a focus on vascular smooth muscle cell (VSMC) contractility is needed to provide targets for anti-hypertensive therapy. The actin cytoskeleton is a dynamic structure that

plays an integral role in generation of mechanical tension and maintenance of vascular patency. Appropriate cytoskeletal organization and protein-protein interactions in proximity to modifying enzymes is essential for VSMC physiological processes, force generation, and regulated vascular contractility.[2] Small GTPases including Cdc42 and Rac1 are major modulators of actin dynamics and cytoskeletal organization and contractility, especially in smooth muscle.[3,4] Attachment of cells to substratum also depends on Cdc42 and Rac1 activation.[3] GTPase abundance and activities are increased in hypertensive arteries, and angiotensin II (AngII), a potent vasoconstrictor, activates Rac1 in SMCs.[5–7] Studies in genetically modified mice show that deletion or overexpression of dominant-negative or dominant-active GTPase or GTPase regulatory proteins induce hypertension or otherwise modify VSMC contractility and blood pressure.[4]

Post-transcriptional mechanisms are an essential response to stimuli and maintenance of homeostasis, as they permit a fine-tuned control of transcript abundance to be rapidly turned on and off as needed.[8] Post-transcriptional regulation of mRNA stability is an understudied yet key mechanism in the regulation of vascular disease, and contractility in particular. There are few examples of the regulation of mRNA stability in VSMCs as a point of control for smooth muscle contraction. RNA-binding proteins including AUF1, hnRNPA1, and HuR have been identified to interact with the AT1R in human VSMCs and modulate its mRNA stability and thus expression.[9,10] HuR deficiency in smooth muscle leads to elevated blood pressure as well as enhanced contraction of VSMCs.[11]

There are interesting examples where regulation of cytoskeletal dynamics and regulation of mRNA stability intersect and potentially have a high impact on VSMC pathophysiological processes. The WASP family verprolin-homologous protein (WAVE) regulatory complex (WRC) is multi-protein complex in the Wiskott-Aldrich syndrome protein (WASP) family involved in the formation of the actin cytoskeleton. Its canonical members include WAVE1, CYFIP1 (cytoplasmic FMR1-interacting protein 1), ABI2, Nap1, and HSPC300, which, through interaction with the Arp2/3 complex (actin related protein 2/3 complex), participate in actin polymerization and rearrangement of the actin cytoskeleton.[12] The WRC is activated by CYFIP1-mediated interaction with Rac1, promoting actin remodeling and cytoskeletal reorganization in a GTP-dependent manner.[13] CYFIP1 and WRC are most associated with chemotaxis, membrane ruffling, and lamellipodia formation and, in combination with Arp2/3 and Rac1, establish neurite polarity and axon outgrowth.[14] There is no literature linking CYFIP1 with VSMCs or vascular disease. Importantly, connections between this complex and regulation of gene expression have been made through interaction of CYFIP1 with eukaryotic translation initiation factor eIF4E and FMRP (fragile X mental retardation protein), which is an RNA-binding protein central to neuronal functioning.[15] Through its protein interactions with eIF4E and FMRP, CYFIP1 is considered to be a component of the translational initiation complex by modification of FMRP affinity for mRNA.

Recently, we identified one FMRP family member, fragile-X-related protein (FXR1), as an RNA-binding protein that, in human VSMCs, reciprocally interacts with and may compete with HuR to regulate transcript stability.[16] FXR1 is a muscle enhanced homolog of FMRP, which is the most studied protein of the FMR family of neuronal proteins.[17,18] FXR1 expression is muscle enhanced, while FMRP and FXR2 are mostly absent in muscle

tissue, causing a number of investigators to ascribe FXR1 as the “muscle homolog” of the much better known FMR1 protein.[19–22] While FXR1 is a muscle-enhanced protein, the artery is mainly composed of VSMCs, and we recently reported that FXR1 expression is increased in atherosclerotic plaque, neointimal SMCs, and tumor necrosis factor α (TNF-α)-stimulated cultured human VSMCs (hVSMCs).[16] Functionally, we found that FXR1 binds to and destabilizes inflammatory and proliferative mRNA transcripts in TNFα-stimulated hVSMCs, which is consistent for a presumed mRNA stability protein. Therefore, FXR1 activity in VSMCs may make an attractive subject of investigation for vascular diseases.

Interestingly, in addition to mRNA-binding domains, FXR1 has five functional domains including an Agenet-like domain for protein-protein interactions.[18,23] Although unreported, we detected that the FXR1 protein also contains four WH2 motif domains that mediates actin interactions and functions as a regulator of actin dynamics and, coincidentally, is also found on WAVE complex proteins. The structure of FXR1 supports its role in post-transcriptional regulation and, though largely ignored, cytoskeletal dynamics via potential protein-protein interactions. With this information in mind, it is reasonable to infer that FXR1 has distinct and essential muscle-specific functions in VSMC pathophysiology, in addition to RNA binding.

Based on this background information, in this article, we test the hypothesis that FXR1 may play a role in VSMC contractility by regulating VSMC cytoskeletal dynamics through regulation of at least two distinct processes: regulation of mRNA stability of cytoskeletal component mRNA and also by mediation of cytoskeletal protein-protein interactions and actin polymerization. Herein, we confirm this hypothesis and show that FXR1 regulates mRNA stability of contractile proteins and also interacts with members of the WRC. Deletion of FXR1 decreases VSMC adherence, motility, contractility and GTPase activation and results in a hypotensive phenotype in FXR1 VSMC-specific conditional knockout mice. When taken together, this points to FXR1 as a muscle-specific WRC component linking mRNA stability and regulation of actin polymerization with VSMC cytoskeletal dynamics, suggesting that FXR1 and its interacting proteins make attractive targets for anti-hypertensive therapy.

RESULTS

FXR1 binds to cytoskeletal, adhesion, and contraction-associated mRNA transcripts

We reported that in primary hVSMCs, FXR1 binds mRNA with a presumed function to modulate its mRNA stability.[16] To identify FXR1-interacting transcripts, FLAG-tagged FXR1 was over expressed in hVSMCs by adenoviral transduction and then immunoprecipitated with anti-FLAG coupled beads. RNA transcripts bound to FXR1 were identified by RNA immunoprecipitation sequencing (RIP-seq) and compared with total mRNA (Data S1). Figure 1A depicts Gene Ontology analysis of the most abundantly bound transcripts compared with total RNA transcripts. Most striking was the highest classification of mRNA transcripts for cell adhesion and matrix organization, processes involved with cytoskeletal dynamics and vascular contractility. Figure 1B is validation of FXR1 knockdown at the protein and mRNA levels in the presence of PDGF-AB, a cytokine recognized to effect VSMC pathophysiology and cytoskeletal arrangements.[24,25]

The effect of FXR1 on abundance of these transcripts as well as expression of other cytoskeletal proteins involved in VSMC pathophysiological processes was determined by qRT-PCR in the presence and absence of PDGF-AB. Figure 1C shows that the mRNA abundance of several of these transcripts, including dynactin, desmoplakin, and filamin B, were significantly decreased when FXR1 was knocked down. To determine FXR1 effects on mRNA stability, hVSMCs were treated with the RNA polymerase inhibitor actinomycin D after PDGF stimulation. Figure 1D shows that the mRNA stability of these transcripts was decreased when FXR1 was reduced by small interfering RNA (siRNA) knockdown. This suggests that the absence of FXR1 affects the stability of several cytoskeletal mRNA transcripts in hVSMCs.

FXR1 regulates actin dynamics and interacts with WAVE complex proteins

Examination of striated muscle in an FXR1 total knockout mouse noted dysregulation of costamere assembly but without a decrease in the abundance of costamere proteins.[20] This suggested that costamere dysregulation in the absence of FXR1 might be a result of absence of FXR1-mediated protein-protein interactions. The Eukaryotic Linear Motif (ELM) database for functional motifs in proteins[26] analysis determined that FXR1 contains four WH2 (WASP-homology 2, or Wiskott-Aldrich homology 2) domain motifs, known to bind to actin and facilitate the assembly of actin monomers into actin filaments, and is found in many WAVE family proteins.[13,27] WH2 is important in cellular processes such as cell contractility, cell motility, cell trafficking, and cell signaling.[15] The relationship between FXR1 and actin dynamics was determined by several complementary experiments. The effect of FXR1 on actin dynamics was investigated first by an actin spin-down assay,[28] in which the ratio of filamentous (F)-actin to globular (G)-actin in hVSMCs lacking FXR1 was determined by quantifying the amounts of each from differential centrifugation.

Figure 2A shows that the ratio of F-actin to G-actin was significantly less in hVSMCs in which FXR1 was depleted by siRNA (42.9% ± 12.1% versus 17.4% ± 5.1% for control versus FXR1 siRNA, $p < 0.05$, respectively), suggesting that FXR1 participates in actin polymerization. Next, hVSMCs were transduced with FLAG-tagged FXR1 to track its actin interaction, and Figure 2B shows that FXR1 sediments with F-actin in the pellet. Furthermore, when the polymerization-enhancing (PE) positive control, 100× phalloidin, is added to the reaction mixture, significantly more FXR1 sediments with F-actin compared with samples lacking phalloidin, reinforcing the notion that FXR1 interacts with F-actin. Actin and other cytoskeletal proteins support cell shape, and Figure 2C shows that hVSMCs depleted of FXR1 by siRNA have altered morphology, with significantly less cells displaying the typical spindle shape indicative of primary cultured hVSMCs and significantly more VSMCs with a polygonal shape.

In addition to WH2 domains, FXR1 contains an Agenet-like functional domain predicted in some proteins to mediate protein-protein interactions, which prompted us to investigate FXR1 protein binding partners in hVSMCs.[29,30] Adenoviral FLAG-tagged FXR1 was immunoprecipitated in hVSMCs, and interacting proteins were identified by mass spectrometric analysis in the presence and absence of RNAse A to rule out protein tethering to mRNA (Data S2). After elimination of non-specific interactions by contaminant

repository for affinity purification (CRAPome) analysis,[31] a role for FXR1 in cytoskeletal dynamics was confirmed by the finding that the largest number of interacting proteins not eliminated by RNAse A treatment were those involved in VSMC cytoskeletal organization and contraction (Figure 3A). The second most abundant proteins were classified as mitochondrial proteins and included primarily mitochondrial 28S ribosomal protein subunits. Several of the cytoskeletal-interacting proteins are members of the WRC, including CYFIP1 or proteins that affiliate with this complex, including Arp2 (Table S1). Since these interactions were not eliminated by RNAse A treatment, they are not co-immunoprecipitated by tethering to FXR1 by mRNA. The WRC is a multi-unit protein complex involved with actin and cytoskeletal dynamics. CYFIP1 has been shown to interact with FMR1 but not FXR1 or its homolog, FXR2.[13,26] Arp2 is part of the Arp2/3 complex and, in concert with the WRC, controls nucleation of actin polymerization and branching of filaments.[32] While it is recognized that the WRC plays a crucial role in cell motility, little has been reported on its participation in VSMC pathophysiological processes. Because of their strong association with actin dynamics, we focused on CYFIP1 and Arp2 for further characterization. PDGF-AB is a well-known stimulator of VSMC cytoskeletal rearrangement, adhesion, and migration.[24] We next determined that FXR1, CYFIP1, and Arp2 expression are increased in PDGF-stimulated hVSMCs (Figures 3B and 3C), suggesting participation of these proteins in PDGF-dependent processes. Interestingly, although its interaction was eliminated by CRAPome analysis, a homolog of FXR1, FXR2, was detected as interacting with FXR1 by mass spectrometry. Although FXR2 is reported to be expressed in coronary artery tissue in GTExPortal and Human Protein Atlas, FXR2 expression did not increase with PDGF-AB stimulation, nor was FXR2 expression affected by FXR1 knockdown; therefore, FXR2 was not further studied (Figure S1).

Direct FXR1 interaction with CYFIP1 and Arp2 was validated by co-immunoprecipitation in the presence of PDGF (Figure 3D). We next used immunocytochemistry to determine FXR1 and Arp2 and CYFIP1 cellular localization under PDGF-stimulated conditions. Figure 3E shows that endogenous FXR1 co-localized with both Arp2 and CYFIP1 primarily in the cytoplasm, which is a region consistent with mRNA processing as well as cytoskeletal-related activities.

Two experiments were performed to determine if actin dynamics played a role in FXR1 interaction with these proteins. First, FXR1 co-immunoprecipitation with Arp2 and CYFIP1 was determined in hVSMCs treated with the actin stabilizer jasplakinolide, which binds to actin and enhances its polymerization.[33] In a second experiment, hVSMCs were treated with the actin destabilizer cytochalasin D, which inhibits actin network formation. Figure 3F shows that, compared with untreated hVSMCs, neither of these drugs appear to affect FXR1-CYFIP1 interaction. However, both jasplakinolide and cytochalasin D appear to enhance FXR1 interaction with Arp2, despite the fact that one drug enhances, and the other destabilizes, actin polymerization. Modification of the concentration of each of these drugs has no effect on these protein-protein interactions (Figure S2). It is possible that while FXR1 can modify actin polymerization, the differences in polymerization state of actin may not result in different interactions of FXR1 with these two proteins. When taken together, these data point to a complex relationship between FXR1 protein-protein interactions, actin polymerization, and the polymerization state of actin.

It has been reported that knocking out one WRC participant can reduce the expression of other subunits, resulting in a reduction of WRC-associated functions.[12] With this in mind, we determined that not only does FXR1 interact with WRC components, but knockdown of FXR1 resulted in significantly less total RNA, mRNA stability, and protein abundance of both Arp2 (Figures 4A and 4B) and CYFIP1 (Figures 4C and 4D) compared with controls. To determine if FXR1 directly interacted with these transcripts, we performed RIP, in which control GFP or FLAG-tagged FXR1 adenovirus was transduced in hVSMCs. FLAG-tagged FXR1 protein was precipitated with immobilized FLAG antibody, and precipitates were subject to RT-PCR in order to identify mRNA transcripts bound to FXR1. FXR1 interacts with both Arp2 and CYFIP1 mRNA (Figures 4A and 4C, respectively). FXR1 directly binds to and regulates Arp2 and CYFIP1 mRNA, and together, these findings suggest that FXR1 is a key regulatory component of the WRC in VSMCs.

GTPase activity is decreased in FXR1-depleted VSMCs

Many of the FXR1-interacting proteins identified by mass spectrometry (MS), as well as FXR1-interacting mRNA transcripts identified by RIP-seq, were associated with G-protein signaling including monomeric GTPases and regulators of G proteins. To test the hypothesis that FXR1 regulates GTPase activity in VSMCs, we utilized a commercially available GTPase activation assay. It was determined that PDGF-stimulated VSMCs in which FXR1 has been knocked down by siRNA have significantly decreased Rac1 and Cdc42 activity compared with control cells (Figure 5A). Interestingly, RNA abundance for each of these GTPases was also reduced when FXR1 was knocked down (Figure 5B). RNA stability of CDC42, but not Rac1, was significantly decreased when FXR1 was knocked down (Figure 5D). Protein abundance of CDC42 was significantly reduced and abundance of Rac1 protein was reduced, but not significantly, in FXR1-depleted hVSMCs, which supports the reduced GTPase activity. Together, these data point to a role for FXR1 in regulation of GTPase activity.

FXR1 regulates VSMC cytoskeleton-dependent activities

It is well accepted that GTPases and GTP exchange activity are essential in actin dynamics regulation, VSMC cytoskeletal organization, and VSMC contractility.[3,4] Cytoskeletal filaments establish and maintain cell shape and function. Their proper abundance and interactions are essential for key cellular events including migration, adhesion, and contractility. With this in mind, several cell-based *in vivo* and *ex vivo* studies were performed to determine that FXR1 regulated VSMC cytoskeletal organization and VSMC contractility. First, hVSMCs depleted of FXR1 by siRNA were grown to confluence in a 4-chamber slide, a uniform scratch was made using a cell scraper, and wound area was quantified 6 h later. Figure 6A shows that in a scratch-wound assay, VSMCs depleted of FXR1 migrate significantly more slowly compared with scrambled siRNA-transfected VSMCs (45.05% ± 6.8% versus 24.62% ± 6.5%, $p < 0.01$, for control and siRNA, respectively). Adherence of the VSMCs to the surface substratum requires a dynamic and fully functioning cytoskeleton. We next determined that hVSMCs depleted of FXR1 adhered significantly more slowly to plastic surface compared with scrambled controls (56.6% and 37.4% for 3 and 6 h, respectively) (Figure 6B). To determine effects on VSMC contraction, we next performed a cell-culture-based VSMC contraction assay in which

hVSMCs were transfected with scrambled control or FXR1 siRNA and then embedded in collagen. Seventy-two hours after, the collagen plug area was quantified.[34] Figure 6C shows that collagen plugs embedded with VSMCs in which FXR1 was depleted contract significantly less compared with scrambled control VSMCs (43.64% ± 2.3% versus 70.08% ± 3.7%. $p < 0.001$ for control and siRNA, respectively). These assays add functional support to the molecular data indicating that FXR1 regulates VSMC function and cytoskeletal organization in VSMCs.

FXR1$^{smc/smc}$ mice are hypotensive

Appropriate actin cytoskeletal dynamics are required for proper muscle tension and vascular contractility, and considering FXR1 expression is muscle enhanced, we hypothesized that deletion of FXR1 from VSMCs would affect blood pressure.[28] FXR1 knockout mice are neonatal lethal with a striated muscle phenotype[12]; therefore, to test the effects of FXR1 depletion *in vivo*, it was necessary to generate a smooth-muscle-specific, FXR1 conditional knockout mouse using the Myh11 promoter (FXR1$^{SMC/SMC}$).[35] Because the Cre gene is on the Y chromosome, only male mice were used in this study. Offspring were healthy and phenotypically normal, and we observed no differences in weight. Figure 7A shows FXR1 expression (red-brown staining) only in endothelium and adventitia of tamoxifen-injected mice. Figure 7B is a western blot indicating that FXR1 expression is greatly reduced in aortic tissue (smooth muscle) and not gastrocnemius tissue (skeletal muscle) in tamoxifen-injected mice. Using telemetric methods, we found that FXR1$^{SMC/SMC}$ mice had significantly decreased mean arterial and diastolic blood pressure when compared with control mice (Figure 7C). Together, this strongly suggests that abrogation of FXR1 expression *in vivo* results in reduced blood pressure.

Aorta in FXR1$^{smc/smc}$ mice have decreased RNA abundance of WAVE proteins and GTPases

To characterize a mechanism for the hypotension observed in the FXR1$^{smc/smc}$ mice, aorta were extracted from vehicle controls (oil) or tamoxifen-injected mice, RNA recovered, and qRT-PCR performed to detect WAVE and GTPase mRNA expression. Reduced FXR1 mRNA abundance confirms that aorta from tamoxifen-injected mice show significantly decreased amounts of FXR1 mRNA (Figure 7D). Figures 7E and 7F show significantly reduced abundance of RAC1 mRNA and protein compared with oil-injected control mice. Figure 7G shows that CYFIP1 mRNA was significantly reduced, and Figure 7H shows that CYFIP1 protein was significantly decreased in tamoxifen-injected compared with vehicle control mice.

To further identify effects of FXR1 deletion *in vivo*, differences in gene expression from aorta pooled from three control mice injected with oil and three injected with tamoxifen were determined using a commercially available PCR array biased to cytoskeletal and cytoskeletal regulatory proteins. Out of 92 genes, 88 of them were significantly decreased (Data S3). Importantly, several of the transcripts identified in this array from aorta of FXR1$^{smc/smc}$ correspond with genes we observed to be reduced when FXR1 was knocked down in hVSMCs, such as Cdc42, Rac1, CYFIP1, and Arp2 (Actr2 on the array). Figure S3 indicates the top 20 decreased genes and the only 4 genes that were increased. This

strongly suggests that *in vivo*, absence of FXR1 results in a reduction in abundance important cytoskeletal protein and GTPases transcripts and may provide a mechanism for the decreased blood pressure observed in FXR1$^{smc/smc}$ mice.

DISCUSSION

Regulation of vascular blood pressure and other cardiovascular processes depend on proper control of VSMC tone. FXR1 is an mRNA stability protein, and although understudied, there are examples of RNA-binding proteins (RBPs) effecting vascular contractility.[9,10] With this in mind, initially, we endeavored to identify FXR1-interacting transcripts by RIP-seq, which pointed to an unexpected preponderance of interactions with transcripts associated with the cytoskeleton. These were validated by qRT-PCR, which demonstrated that FXR1 affects the mRNA stability of multiple cytoskeletal proteins that participate in cellular functions ranging from maintenance of cell shape, migration, and force generation. Like many mRNA-binding proteins, FXR1 interacts with specific elements in mRNA and is known to interact with mRNA via ATTTA (ARE-rich element) in the 3′ UTR of many mRNA transcripts so that any cytoskeletal transcript with an ARE has the potential to be recognized by FXR1.[16] This is also consistent with a report indicating that FXR1 knockout affects costamere assembly in striated muscle.[20]

The WH2 domain is an ~18-amino-acid actin-binding motif that functions as a regulator of actin dynamics and is present in proteins that participate in important cellular processes such as cell contractility and motility.[12,14] This domain was first recognized as an essential element for the regulation of the cytoskeleton by WAVE family members. Functional motif analysis identified four WH2 domains in FXR1, which are known to mediate actin interactions and facilitate the assembly of actin monomers into actin filaments.[13,27] This information, together with FXR1's muscle-enhanced expression, prompted us to investigate if FXR1 interacted with and modified actin polymerization in hVSMCs. The present study demonstrates that FXR1 directly interacts with actin, and depletion of FXR1 from hVSMCs resulted in less F-actin compared with controls, suggesting that FXR1 is a participant in the regulation of actin dynamics.

The pan-FXR1 knockout mouse is lethal within hours of birth,[20] which the authors attributed to a dysregulated costamere appearance in striated muscle (smooth muscle was not examined) in the newborn pups. Costameres are a structural and functional component of striated muscle cells responsible for contractile force by coupling myofibrils to the sarcolemma. The authors of this study showed that while muscle from *FXR1*$^{-/-}$ mice contained normal amounts of costameric proteins, the structure of striated muscle costameres was dysregulated, but no mechanism was offered for this observation. While smooth muscle does contain some costamere proteins, they do not contain recognized costamere structures. FXR1 co-immunoprecipitates with actin, and depletion of FXR1 from hVSMCs resulted in less F-actin. FXR1 contains an Agenet domain, recognized in the FMR1 protein to regulate protein-protein interactions.[36,37] Even though FXR1 contains an Agenet domain, very little has been published concerning FXR1 protein-protein interactions. This information, together with the dysregulated costamere structure noted in the total knockout mouse, prompted us to investigate FXR1 protein interactions in VSMCs by MS.

MS indicated and co-immunoprecipitation validated that FXR1 directly interacted with CYFIP1, a member of the WRC, and Arp2, known to interact with the WRC, which together regulate actin cytoskeletal dynamics. In its canonical form, the WRC consists of 5 conserved WASP family proteins including WAVE1, CYFIP1, ABI2, Nap1, and HSPC300. We did not detect FXR1 interaction with these other WRC proteins by MS. CYFIP1 expression and function has not been reported in VSMCs, but in neurons, it plays a unique function linking mRNA metabolism with actin remodeling.[38] CYFIP1 has been reported to interact with FMR1[39] but to the exclusion of FXR1 and FXR2, so our study does not concur with the literature, likely because most studies focusing on FMR1 utilize neuronal cells or cancer cell lines rather than primary hVSMCs and other muscle types where FXR1 is highly expressed. Furthermore, the observation that actin polymerization as well as depolymerization can enhance FXR1 interaction with Arp2, while not affecting its interaction with CYFIP1, may not be surprising, as Arp2 is a key regulator of actin dynamics. This does indicate a complex relationship between the ability of FXR1 to affect actin polymerization and how the polymerization state of actin can affect FXR1 protein-protein interactions with different proteins.

While never reported for FXR1, CYFIP2 mRNA is a target of FMRP, which is known to modulate its expression.[40] Further, it is known that suppression of expression of one or more components of the WRC reduces expression of other subunits. One likely mechanism is that CYFIP1 has been shown to interact with translation initiation factor eIF4E, which, similar to FXR1, participates in mRNA metabolism.[40] In concordance with these observations, knockdown of FXR1 resulted in decreased expression of both CYFIP1 and ARP2. It has been shown that in neuronal cells, FMRP can regulate the expression of cytoskeletal proteins,[41–43] suggesting that this may be a likely mechanism for our observations that FXR1 knockdown decreased the mRNA stability of several cytoskeletal proteins. When taken together, this indicates that FXR1 may regulate VSMC cytoskeletal dynamics by two mechanisms: first, as a participant in the WRC, and second, by regulation of cytoskeletal mRNA stability and abundance of these important proteins.

Small GTPases, including Cdc42, and Rac1 are major modulators of actin dynamics and cytoskeletal organization and contractility, especially in smooth muscle.[3,4] Importantly, members of the WRC can act cooperatively with GTPases to activate the Arp2/3 complex to polymerize actin.[12,44] In fact, it is believed CYFIP1 provides the binding site for the WRC to interact with Rac1 which allows it to modify cytoskeletal dynamics.[27,45] In our study in hVSMCs, FXR1 knockdown significantly reduces both Rac1 and CDC42 activity, which would have important implications on several VSMC pathophysiological processes, including adhesion, migration, and contractility, all activities known to involve these GTPases. FXR1, Arp2, and CYFIP1 expression are increased by stimulation of PDGF-AB, a cytokine known to modify actin dynamics and dependent activities such as migration and adhesion.[24] In SMCs, actin filaments connect the membrane with cytoplasmic dense plaques so that actin polymerization can influence force development. In this study, we demonstrated that VSMC contraction, migration, and cell adhesion are all significantly reduced in FXR1-depleted hVSMCs. Each of these processes depends on GTPase and WRC activity, further associating FXR1 with important cytoskeletal-associated activities.

There is literature linking the WRC with membrane protrusion and cell migration in cancer cells and neurons but little reporting an association of this complex with VSMC contractility. Although it has been reported that activated Cdc42 triggers actin polymerization and SMC contraction,[46] the role of Rac1 in VSMC contraction is less clear, with some reports suggesting antagonism to contractile agents and others showing enhancement of contraction.[4] Nevertheless, GTPase abundance and activities are increased in hypertensive arteries,[5,7] and AngII activates Rac1 in SMCs. We next determined in a collagen-based contraction assay that hVSMCs depleted of FXR1 contract significantly less than scrambled controls. This can be attributed to decreased GTPase activity and/or dysregulated expression of WRC and other cytoskeletal proteins. In this study, we have shown the involvement of FXR1 in hVSMC contractility, and this corroborates the RIP-seq and MS data linking FXR1 as a participant in cytoskeletal regulation.

Studies in genetically modified mice show that deletion or overexpression of dominant-negative or dominant-active GTPase or GTPase regulatory proteins induce hypertension or otherwise modify VSMC contractility and blood pressure *in vivo*.[4] These studies include some proteins that interacted with FXR1 as determined by MS, including ARHgef and Rock1. Knockouts of either of these noted no change in basal blood pressure.[5,47]

This information raised the question that FXR1 deletion in VSMCs might modify blood pressure *in vivo*. Because FXR1 knockout mice are neonatal lethal, it was necessary to generate smooth-muscle-specific FXR1 conditional knockout mice. While these mice were normal in appearance, telemetry demonstrated that at basal conditions, mice lacking FXR1 in VSMCs had significantly lower mean arterial and diastolic blood pressure compared with control populations. Future studies should determine the effect of FXR1 deletion in established models of hypertension such as AngII infusion. In the search for potential mechanisms of this effect, we next looked at expression of WRC proteins and GTPases in aorta from these mice. Importantly, mRNA and protein for Rac1 and CYFIP1 were significantly reduced.

To further identify effects of FXR1 deletion *in vivo*, we utilizeda commercially available PCR array biased to cytoskeleton and cytoskeletal regulatory proteins and compared gene expression in aorta pooled from three oil- and tamoxifen-injected mice each. Most striking was that the majority of mRNA transcripts (88 of 92 tested) were significantly decreased. Notably, transcripts such as Arp2, CYFIP1, Rac1, and Cdc42, which were identified as reduced in hVSMCs with FXR1 siRNA, were also significantly reduced in aorta from tamoxifen-injected mice, validating those results and demonstrating conservation of effect across species. Importantly, mRNA from members in the WRC family, including WAS, WASl, and WASf1 (Wiskott-Aldrich syndrome, Wiskott-Aldrich like, and WASP family 1, respectively) were also significantly reduced. Other transcripts that were reduced included those that modified small GTPase, microtubule-associated, and structural proteins. We surmise that the decreased expression of these genes in aorta lacking FXR1 may account for the hypotension observed *in vivo*.

There is no literature associating FXR1, CYFIP1, Arp2, and WRC proteins in regulation of vascular contractility. Although there are reports linking the WRC and Arp2 with

cytoskeletal activities, they are in the context of cancer cell metastasis and neuronal sprouting. There is no literature associating the WRC or CYFIP1 expression or function with VSMC contraction or blood pressure regulation. Similarly, the Arp2/3 complex participates in actin polymerization and cytoskeletal dynamics. There is one report suggesting that Cdc42 activation of the Arp2/3 complex results in actin polymerization and contractility in airway smooth muscle, but FXR1 involvement is not mentioned.[48]

In summary, we posit that there are two potential mechanisms for reduced contractility in cultured FXR1-depleted VSMCs and vascular hypotension *in vivo* in $FXR1^{SMC/SMC}$. The first is transcriptional; since FXR1 is an mRNA stability protein, deletion of FXR1 results in a reduction in abundance of cytoskeletal proteins, resulting in inadequate amounts of contractile machinery to effectively generate force or movement. The second mechanism is facilitated by FXR1-mediated protein-protein interactions. Deletion of FXR1 results in reduced actin polymerization and interactions with WRC components. Together, this points to FXR1 as a muscle-enhanced, integral component of the WRC and an important regulator of VSMC cytoskeletal dynamics and vascular contractility. This work also suggests that FXR1 and WRC component proteins may represent targets for anti-hypertensive therapy.

Limitations of study

There are limitations to this study that require further investigation. At the molecular level, mutational analysis of pertinent domains in the FXR1 protein that mediate mRNA binding and protein-protein interactions could add insight into the primary mechanism(s) by which FXR1 mediates its effects on the cytoskeleton. It would be important to determine protein-protein interactions of FXR1 with WAVE proteins in arteries, which are involved in the regulation of blood pressure. Determination of blood pressure in $FXR1^{SMC/SMC}$ mice in a recognized model of hypertension, such as AngII infusion or a high-salt diet, would add additional translational consequences to this study.

STAR★METHODS

RESOURCE AVAILABILITY

Lead contact—Further information and requests for resources and reagents should be directed to and will be fulfilled by the lead contact, Michael Autieri, PhD (mautieri@temple.edu).

Materials availability—FXR1 conditional smooth muscle knock out mice will be shared from the lead contact upon reasonable request. Otherwise, this study did not generate new unique requests.

Data and code availability

- RNA immunopreciptation sequencing data and mass spectrometry data have not been deposited as they are available in the manuscript.
- This paper does not report original code.

- Any additional information required to reanalyze the data reported in this paper is available from the lead contact upon request.

EXPERIMENTAL MODEL AND SUBJECT DETAILS

VSMC culture—Primary human coronary artery vascular smooth muscle cells from male donors were obtained as cryopreserved secondary culture from Lonza Corporation [Allendale, NJ, USA] and maintained as we described.[16,49] Male donors were used to match the mouse study, where the FXR1 conditional knock out model is Y-linked. Cells were incubated at 37C and 5% CO_2. Cells were used from passage 3–5.

Mouse model and telemetry—Floxed FXR1 mice were obtained from the from the Fragile X Research Foundation (fraxa.org/fragile-x0research/resources) and described in.[20] Briefly, this mouse carries *loxP* sites that were introduced by homologous recombination to flank the promoter and first exon of Fxr1. This mouse was crossed with an SMC-specific Cre driver (SmMHC-CreER^{T2}) which carries the Cre transgene on the Y chromosome,[35] therefore only male mice are used in this study. Breeding was standard harem breeding of two female mice to one male mouse. Mice were phenotypically normal, and had no significant differences in weights between control and tamoxifen-injected mice. Blood pressure assessment by radio-telemetry was performed as we described.[50] Briefly, eight- to ten-week-old male FXR1 F/F, tamoxifen-inducible, conditional FXR1$^{VSMC/VSMC}$, and SMC-specific cre driver (SmMHC-CreER^{T2}) mice received 5 days of i.p oil or tamoxifen injections (80 μg/kg) followed by a one week washout. All mice were anesthetized by isoflurane inhalation (induction dose: 3–5%, maintenance dose: 1–2%) received radiometric telemeter implants where the catheter of the telemeter is inserted into the left carotid artery via carotid catheter (PA-C10 transmitter) and then fed down to the aortic arch. Telemetric readings of systolic, diastolic and mean blood pressure (mmHg) were measured for 26 h and analyzed using Ponemah software (Data Science International). In the analysis, the first and last hour of the reading were removed to eliminate potential false readings due to experimenter disruption. All animal procedures were performed following Temple University Animal Care and Use Committee approved protocols.

METHOD DETAILS

RNA immunoprecipitation qRT-PCR and sequencing—HVSMC were transduced with flag-tagged adenoviral FXR1 and either serum starved for 24 h and stimulated with 10 ng/mL of TNFa for 6 h or unstimulated as control. Cells were collected and lysed in buffer containing 0.1M Tris-HCL; pH 8.5, 50 mM HEPES; pH 7.5, 70mM potassium acetate, and 5 mM magnesium acetate and rocked on a nutator at 4°C for 30 min. Samples were centrifuged for 15 min at 4°C. Supernatant was added to either anti-flag M2 affinity gel beads (Sigma-Aldrich, St. Louis, MO, USA) or control protein A/G PLUS agarose beads (Santa Cruz Biotechnology, Inc., Dallas, TX, USA) and incubated for 4 h at 4°C on nutator. Beads were then spun down, washed, and trizol was added. RNA was isolated and Library preparation and unbiased RNA sequencing was performed by GeneWiz, (South Plainfield, NJ). libraries were sequenced using a 1 × 100-bp single end rapid run on the HiSeq2500 platform, and a comparison of gene expression using DESeq2. The Wald test was used to generate p values and log2 fold changes. Genes with a p value <0.05 and absolute log2 fold

change >1 were called differentially expressed genes. Significantly differentially expressed genes were clustered by their gene ontology and the enrichment of gene ontology terms was tested using Fisher exact test (GeneSCF v1.1-p2). Log2(Group 2 mean normalized counts/Group 1 mean normalized counts) = Log2FoldChange. Some immunoprecipitates were subject to reverse transcription and PCR using specific primers as described in a following section.

LC-MS/MS. LC-MS/MS—LC-MS/MS analysis was performed as described previously.[16,51] Briefly, VSMC were transduced with recombinant adenovirus expressing FLAG-tagged HuR or empty vector control. Pellets were collected and lysed in maltoside based-lysis buffer containing 1× protease inhibitor tablet (Roche) for 30 min on a nutator at 4°C. The lysates were centrifuged at 16,600 × *g* for 15 min to remove cell debris, and the supernatant was incubated with anti-FLAG beads, followed by 5 washes in lysis buffer. Proteins were eluted from beads in 10 M freshly prepared urea. Digestion was performed in 100 mM Tris-HCl (pH 8.5) containing 8 M urea at 37°C first with Lys-C (35 ng/mg lysate) for 4 h, and then the urea concentration was reduced to 2 M for trypsin (30 ng/mg lysate) digestion overnight. Following digestion, the tryptic peptides were desalted on a reversed-phase Vivapure C18 micro spin column (Sartorius Stedim Biotech, Gottingen, Germany) and concentrated using a SpeedVac. Dried samples were acidified by 0.2% formic acid prior to liquid chromatography-mass spectrometric analysis. All LC-MS/MS experiments were performed on a nanoflow LC system, EASY-nLC II (Thermo Scientific, Waltham, MA, USA) connected to a hybrid LTQ Orbitrap Classic (Thermo Scientific, Waltham, MA, USA) equipped with a nano-electrospray ion source. For the EASY-nLC II system, solvent A consisted of 97.8% H2O, 2% ACN, and 0.2% formic acid and solvent B consisted of 19.8% H2O, 80% ACN, and 0.2% formic acid. Samples were directly loaded onto a 16-cm analytical HPLC column (75 mm ID) packed in-house with ReproSil-Pur C18AQ 3 μm resin (120A° pore size, Dr. Maisch, Ammerbuch, Germany). The column was heated to 45°C. The peptides were separated with a 160 min gradient at a flow rate of 350 mL/min. The gradient was as follows: 2–30% Solvent B (150 min), 30–100% B (1 min), and 100% B (9 min). Eluted peptides were then ionized using a standard coated silica tip (New Objective, Woburn, MA, USA) as an electrospray emitter and introduced into the mass spectrometer. The LTQ Orbitrap was operated in a data-dependent mode, automatically alternating between a full-scan (m/z 300–1700) in the Orbitrap and subsequent MS/MS scans of the 15 most abundant peaks in the linear ion trap (Top15 method). Data acquisition was controlled by Xcalibur 2.0.7 and Tune 2.4 software (Thermo Fisher Scientific, Waltham, MA, USA). For data analysis, peaks were generated from raw data files using MaxQuant (version 1.5.1.2) with default parameters and searched using the built-in search engine Andromeda. Peak lists were searched against the UniProt human database (148298 sequences including isoforms) and a contaminant database (262 sequences). Thresholds for peptide and protein scores were chosen to have at most a 1% FDR as estimated by a decoy database.[52,53]

RNA Extraction and quantitative RT-PCR and mRNA stability—VSMCs were serum starved in 0.2% FCS for 48 h, then stimulated with 40 ng/mL PDGF-AB for the indicated times. RNA from cultured VSMCs was isolated and reverse transcribed into

cDNA, as we have described, and target genes were amplified using an Applied Biosystems StepOne Plus Real-Time PCR System as we described.[16,54,55] Multiple mRNAs (CT values) were quantitated simultaneously by the Applied Biosystems software. Primer pairs were purchased from Integrated DNA Technologies (Coralville, IA, USA), and SYBR Green was used for detection. Messenger RNA stability was performed as we described.[16,56] Briefly, samples were treated with 40 ng/mL of PDGF-AB for 16 h, 10 μg/ml of the transcription inhibitor Actinomycin D was added and RNA extracted at indicated time points after stimulation.

The following primer pairs were used:

Human: Forward Reverse

GAPDH CGAGAGTCAGCCGCATCTT, CCCCATGGTGTCTGAGCG, FXR1 GAGTTACCGCCATTGAGCTAG, ACTTTTCCAACGAGATTCCTAGG

RAC1	**CCTGTAGTCGCTTTGCCTATT**	**CTCGCCAGTGAGTTAAGTTGTA**
CDC42	CCTGGCTCCCTTCTTTCATTAG	CATGAGTATCCCTGACCGTTTG
RhoA	CATGGAGCTGGGCTAAGTAAA	GTCCAGGTGAGACAGGTTATG
ARP2	TAGTGGTAGACTCTGGAGATGG	CGTATCCTCGCAACAGAAGTAG
Cortactin	CGGTATCGACAAGGACAAAGT	TCCTCCAAACCCTTTCACATAG
Dynactin	GGCAGAGAAGGCAGAACTAAA	CCAGAGTAGCAATGCCTGAA
CYFIP1	TTCCAGGCATCATGGGATTAG	CTGAGCATTCGATGGCCTTA
Filamin B	CCCTCGCTCTGGTGATTATTT	AAGGGACTGAAACGGACTTG
Desmoplakin	GACTCCAAGCAGAGATCAAGAG	CGGGAGCGTTCTGTTTCTAA
ACTG1	CCTCTTCCAGCCTTCCTTTATT	AGTCCTTACGGATGTCAATGTC
Mouse	**Forward**	**Reverse**
GADPH	GGAGAAACCTGCCAAGTATGA	TCCTCAGTGTAGCCCAAGA
FXR1	GAACGCATGGCAGTAACATAC	CACAAATTCCAAGAAACCTCTAGC
RAC1	AGAGATCGGTGCTGTCAAATAC	CTCGGATAGCTTCGTCAAACA
CDC42	ATGATTGGTGGAGAGCCATAC	GATGGAGAGACCACTGAGAAAC
RhoA	ACCAGTTCCCAGAGGTCTAT	GTCCAGCT GTGTCCCATAAA
Mouse	**Forward**	**Reverse**
ARP2	CAGTCACAGTGGAATCCCTAAG	TCCTATGCACAGCAGGTAATG
Cortactin	AGTGTTTGGAAGAGGAGGAAAG	AGTGGTCAGGACTGACAGATA
Dynactin	GTGCAGTGTGGACGTGTATAA	CTCGGAGAAGAAGGGCAATATC
CYFIP1	GTGTCTGCACCTTATGGAAGA	CCGGTTGGTAGAGCCATTATAG
Filamin B	GACAGAGGAAACCAGGTGTATAG	AAAGGGACTCTTGGGAATGG
Desmoplakin	TGTCTCGGATGGCTACTTAAAC	CCAGACAGACAGTTTCCTCTTC
ACTG1	CACTCCTTCTTGCCAGTCTAAC	TCCCAACTCAAGGCAACTAAC

PCR array—Differences in gene expression from aorta pooled from three control mice injected with oil and three injected with tamoxifen was achieved using the biased RT2 Profiler PCR Array Mouse Cytoskeleton Regulators Cat# PAMM-049Z from Qiagen as described by the manufacturer.

Transfection, siRNA knockdown and overexpression—Gene silencing was performed using ON-TARGET plus SMARTpool FXR1 siRNA, which contains a mixture of four siRNAs which target human FXR1 (10 nM) purchased from Dharmacon, Inc. (Lafayette, Co, USA) as we have described.[16,54,57] Scrambled control siRNA was also purchased from Dharmacon, Inc. Transfection of VSMC was performed using the AMAXA Nucleofector Kit (Amaxa, Inc., Gaithersburg, MD, USA) following the manufacturer's instructions as we described.[16,49,54] For overexpression studies, adenovirus vector encoding human FXR1 cDNA (AdFXR1) and control GFP was purchased from Vigene Biosciences (Rockville, MD, USA). The AdenoFXR1 and control virus AdenoGFP were used at 100 MOI in the transduction of hVSMCs. Forty-eight hours after infections, VSMC were serum starved 24 h, then treated as described in the legend.

Western blotting and protein determination—Human VSMC extracts were prepared as described.[16,54,58] Membranes were incubated with a 1:2000–9000 dilution of primary antibody, and a 1:5000 dilution of secondary antibody. FXR1, CYFIP1 and Glyceraldehyde 3-phosphate dehydrogenase (GAPDH) were from Cell Signaling (Danvers, MA, USA), FXR2 antibody from GeneTex (Irvine, CA USA). FLAG, ARP2 and CDC42 antibodies were from Proteintech (Rosemonth, IL USA). RAC1 antibody was from Abcam (Boston, MA USA).Human antigen Reactive proteins were visualized using enhanced chemiluminescence (Amersham, Piscataway, NJ, USA) according to manufacturer's instructions. Relative intensity of bands was normalized to GAPDH, and quantitated by scanning image analysis and the ImageJ densitometry program.

Co-immunoprecipitation—Co-immunoprecipitation and was performed as we described.[16,54] Briefly, hVSMCs were washed three times in PBS and scraped off the dish into a conical tube and centrifuged to form cell pellet. HVSMC extracts were lysed in Lysis Buffer (50mM HEPES, pH 7.5, 70mM KOAc, 5 mM Mg(OAc)2 in 0.1M Tris-HCl, pH 8.5 with 0.1g n-dodecyl-B-Maltoside and protease inhibitor) and incubated on a nutator at 4°C for 30 min with the addition of RNAse A to eliminate the possibility of tethering on mRNA. Cells were centrifuged at 16,600K for 15 min. Anti-FLAG M2 Affinity beads (Sigma Aldrich, St. Louis, MO, USA) were washed and added to each sample and incubated on the nutator overnight at 4°C. The samples were centrifuged at 13,000rpm and washed three times in lysis buffer. Sample buffer was added and samples were boiled and frozen or used for western blotting. In some samples, the actin modification compounds jasplakinolide (0.5μM) and cytochalasin D (2μM) were added to hVSMC cultures 30 min prior to cell collection. Co-immunoprecipitation proceeded as described above.

Collagen gel contraction—The collagen gel contraction assay provides a cell culture model for tissue contraction based on the fact that cell-populated collagen hydrogels contract over time in a predictable and consistent manner. 1 $X10^5$ of human VSMCs with were

suspended into collagen gels made of Rat Tail Type 1 collagen as described.[34] Collagen gels were photographed after 72 h and gel surface area was calculated by ImageJ.

Scratch wound and adhesion assay—VSMC scratch wounding was performed as we described.[59] Human VSMCs were plated in a 4-well chamber slide in triplicate and 48 h after transfection, a 2-mm uniform scratch was made. Images were taken immediately after scratch and 24 h after scratch using EVOS M5000 at 4X (Invitrogen). Migration into the area devoid of cells were quantified using ImageJ as a percentage of control. For VSMC adhesion, after transfection, hVSMCs were plated into a 24-well tray (10,000/well) 48 h after transfection. Adherent cells were trypsinized and counted at 3 and 6 h.

Actin polymerization and actin binding—Effects of FXR1 on actin dynamics determined by a kit from Cytoskeleton, Inc (cat# BK037) according to manufacturer's instructions. Briefly, hVSMC treated with FXR1 siRNA, scrambled control, AdFXR1 or AdGFP were lysed in actin stabilization buffer. The general approach is to homogenize cells in F-actin stabilization buffer, followed by centrifugation to separate the F-actin from G-actin pool. In some samples F-actin Enhancing Solution (100x phalloidin stock) was added to drive polymerization and actin pelleting. The fractions are then separated by SDS-PAGE and actin is quantitated by Western blot as described.[28] The final result gives an accurate method of determining the ratio of F-actin incorporated into the cytoskeleton versus the G-actin found in the cytosol.

GTPase activity—CDC42 and RAC1 activity levels were measured by ELISA (G-LISA Cytoskeleton #153BK). In brief, the kit contains the respective GTP-binding protein linked to the plate and active bound GTPase in cell/tissue lysates will bind to the wells. The bound active GTPase is detected with a GTPase specific antibody. Finally, the plate was developed with a colorimetric substrate and absorbance read at 490nm.

Mice and telemetry—Floxed FXR1 mice were obtained from the from the Fragile X Research Foundation (fraxa.org/fragile-x0research/resources) and described in.[20] Briefly, this mouse carries *loxP* sites that were introduced by homologous recombination to flank the promoter and first exon of Fxr1. This mouse was crossed with an SMC-specific Cre driver (SmMHC-CreER^{T2}) which carries the Cre transgene on the Y chromosome.[35] Breeding was standard harem breeding of two female mice to to one male mouse. Mice were phenotypically normal, and had no significant differences in weights between control and tamoxifen-injected mice. Blood pressure assessment by radio-telemetry was performed as we described.[50] Briefly, eight-to ten-week-old male FXR1 F/F, tamoxifen-inducible, conditional FXR1$^{VSMC/VSMC}$, and SMC-specific cre driver (SmMHC-CreER^{T2}) mice received 5 days of i.p oil or tamoxifen injections (80 μg/kg) followed by a one week washout. All mice were anesthetized by isoflurane inhalation (induction dose: 3–5%, maintenance dose: 1–2%) received radiometric telemeter implants where the catheter of the telemeter is inserted into the left carotid artery via carotid catheter (PA-C10 transmitter) and then fed down to the aortic arch. Telemetric readings of systolic, diastolic and mean blood pressure (mmHg) were measured for 26 h and analyzed using Ponemah software (Data Science International). In the analysis, the first and last hour of the reading were removed

to eliminate potential false readings due to experimenter disruption. All animal procedures were performed following Temple University Animal Care and Use Committee approved protocols.

QUANTIFICATION AND STATISTICAL ANALYSIS

Results are expressed as mean ± SD. Differences between groups were evaluated with the use of Student's t-test, or ANOVA for multiple comparisons using GraphPad Prism (version 8.0), where appropriate. Differences were considered significant when $p < 0.05$. Statistical details of experiments can be found in the figure legends.

Supplementary Material

Refer to Web version on PubMed Central for supplementary material.

ACKNOWLEDGMENTS

This work was supported by grants from the National Heart, Lung, and Blood Institute of the National Institutes of Health (HL141108 and HL117724 to M.V.A. and HL160211 to A.S.P.).

REFERENCES

1. Blacher J, Evans A, Arveiler D, Amouyel P, Ferrières J, Bingham A, Yarnell J, Haas B, Montaye M, Ruidavets JB, et al. (2010). Residual cardiovascular risk in treated hypertension and hyperlipidaemia: the PRIME Study. J. Hum. Hypertens. 24, 19–26. 10.1038/jhh.2009.34. [PubMed: 19474798]
2. Gunst SJ, and Zhang W (2008). Actin cytoskeletal dynamics in smooth muscle: a new paradigm for the regulation of smooth muscle contraction. Am. J. Physiol. Cell Physiol. 295, C576–C587. 10.1152/ajp-cell.00253.2008. [PubMed: 18596210]
3. van Nieuw Amerongen GP, and van Hinsbergh VW (2001). Cytoskeletal effects of rho-like small guanine nucleotide-binding proteins in the vascular system. Arterioscler. Thromb. Vasc. Biol. 21, 300–311. 10.1161/01.atv.21.3.300. [PubMed: 11231907]
4. Loirand G, and Pacaud P (2010). The role of Rho protein signaling in hypertension. Nat. Rev. Cardiol. 7, 637–647. 10.1038/nrcar-dio.2010.136. [PubMed: 20808285]
5. Seko T, Ito M, Kureishi Y, Okamoto R, Moriki N, Onishi K, Isaka N, Hartshorne DJ, and Nakano T (2003). Activation of RhoA and inhibition of myosin phosphatase as important components in hypertension in vascular smooth muscle. Circ. Res. 92, 411–418. 10.1161/01.RES.0000059987.90200.44. [PubMed: 12600888]
6. Mukai Y, Shimokawa H, Matoba T, Kandabashi T, Satoh S, Hiroki J, Kaibuchi K, and Takeshita A (2001). Involvement of Rho-kinase in hypertensive vascular disease: a novel therapeutic target in hypertension. FASEB J Off Publ Fed Am Soc Exp Biol 15, 1062–1064. 10.1096/fj.00-0735fje.
7. Denniss SG, Jeffery AJ, and Rush JWE (2010). RhoA-Rho kinase signaling mediates endothelium- and endoperoxide-dependent contractile activities characteristic of hypertensive vascular dysfunction. Am. J. Physiol. Heart Circ. Physiol. 298, H1391–H1405. 10.1152/ajpheart.01233.2009. [PubMed: 20154258]
8. Schoenberg DR, and Maquat LE (2012). Regulation of cytoplasmic mRNA decay. Nat. Rev. Genet. 13, 246–259. 10.1038/nrg3160. [PubMed: 22392217]
9. van der Veer EP, de Bruin RG, Kraaijeveld AO, de Vries MR, Bot I, Pera T, Segers FM, Trompet S, van Gils JM, Roeten MK, et al. (2013). Quaking, an RNA-binding protein, is a critical regulator of vascular smooth muscle cell phenotype. Circ. Res. 113, 1065–1075. 10.1161/CIRCRESAHA.113.301302. [PubMed: 23963726]

10. Li F, Hu DY, Liu S, Mahavadi S, Yen W, Murthy KS, Khalili K, and Hu W (2010). RNA-binding protein HuR regulates RGS4 mRNA stability in rabbit colonic smooth muscle cells. Am. J. Physiol. Cell Physiol. 299, C1418–C1429. 10.1152/ajpcell.00093.2010. [PubMed: 20881234]

11. Liu S, Jiang X, Lu H, Xing M, Qiao Y, Zhang C, and Zhang W (2020). HuR (human antigen R) regulates the contraction of vascular smooth muscle and maintains blood pressure. Arterioscler. Thromb. Vasc. Biol. 40, 943–957. 10.1161/ATVBAHA.119.313897. [PubMed: 32075416]

12. Rottner K, Stradal TEB, and Chen B (2021). WAVE regulatory complex. Curr. Biol. 31, R512–R517. 10.1016/j.cub.2021.01.086. [PubMed: 34033782]

13. Chen Z, Borek D, Padrick SB, Gomez TS, Metlagel Z, Ismail AM, Umetani J, Billadeau DD, Otwinowski Z, and Rosen MK (2010). Structure and control of the actin regulatory WAVE complex. Nature 468, 533–538. 10.1038/nature09623. [PubMed: 21107423]

14. Schaks M, Giannone G, and Rottner K (2019). Actin dynamics in cell migration. Essays Biochem. 63, 483–495. 10.1042/EBC20190015. [PubMed: 31551324]

15. Abekhoukh S, and Bardoni B (2014). CYFIP family proteins between autism and intellectual disability: links with Fragile X syndrome. Front. Cell. Neurosci. 8, 81. 10.3389/fncel.2014.00081. [PubMed: 24733999]

16. Herman AB, Vrakas CN, Ray M, Kelemen SE, Sweredoski MJ, Moradian A, Haines DS, and Autieri MV (2018). FXR1 is an IL-19-responsive RNA-binding protein that destabilizes pro-inflammatory transcripts in vascular smooth muscle cells. Cell Rep. 24, 1176–1189. 10.1016/j.celrep.2018.07.002. [PubMed: 30067974]

17. Devys D, Lutz Y, Rouyer N, Bellocq JP, and Mandel JL (1993). The FMR-1 protein is cytoplasmic, most abundant in neurons and appears normal in carriers of a fragile X premutation. Nat. Genet. 4, 335–340. 10.1038/ng0893-335. [PubMed: 8401578]

18. Bardoni B, Schenck A, and Mandel JL (2001). The Fragile X mental retardation protein. Brain Res. Bull. 56, 375–382. [PubMed: 11719275]

19. Garnon J, Lachance C, Di Marco S, Hel Z, Marion D, Ruiz MC, Newkirk MM, Khandjian EW, and Radzioch D (2005). Fragile X-related protein FXR1P regulates proinflammatory cytokine tumor necrosis factor expression at the post-transcriptional level. J. Biol. Chem. 280, 5750–5763. 10.1074/jbc.M401988200. [PubMed: 15548538]

20. Mientjes EJ, Willemsen R, Kirkpatrick LL, Nieuwenhuizen IM, Hoogeveen-Westerveld M, Verweij M, Reis S, Bardoni B, Hoogeveen AT, Oostra BA, and Nelson DL (2004). Fxr1 knockout mice show a striated muscle phenotype: implications for Fxr1p function *in vivo*. Hum. Mol. Genet. 13, 1291–1302. 10.1093/hmg/ddh150. [PubMed: 15128702]

21. Khandjian EW, Fortin A, Thibodeau A, Tremblay S, Côté F, Devys D, Mandel JL, and Rousseau F (1995). A heterogeneous set of FMR1 proteins is widely distributed in mouse tissues and is modulated in cell culture. Hum. Mol. Genet. 4, 783–789. 10.1093/hmg/4.5.783. [PubMed: 7633436]

22. Coy JF, Sedlacek Z, Bächner D, Hameister H, Joos S, Lichter P, Delius H, and Poustka A (1995). Highly conserved 3' UTR and expression pattern of FXR1 points to a divergent gene regulation of FXR1 and FMR1. Hum. Mol. Genet. 4, 2209–2218. 10.1093/hmg/4.12.2209. [PubMed: 8634689]

23. Bechara E, Davidovic L, Melko M, Bensaid M, Tremblay S, Grosgeorge J, Khandjian EW, Lalli E, and Bardoni B (2007). Fragile X related protein 1 isoforms differentially modulate the affinity of fragile X mental retardation protein for G-quartet RNA structure. Nucleic Acids Res. 35, 299–306. 10.1093/nar/gkl1021. [PubMed: 17170008]

24. Abedi H, and Zachary I (1995). Signalling mechanisms in the regulation of vascular cell migration. Cardiovasc. Res. 30, 544–556. [PubMed: 8575003]

25. Hughes AD, Clunn GF, Refson J, and Demoliou-Mason C (1996). Platelet-derived growth factor (PDGF): actions and mechanisms in vascular smooth muscle. Gen. Pharmacol. 27, 1079–1089. 10.1016/s0306-3623(96)00060-2. [PubMed: 8981052]

26. Kumar M, Michael S, Alvarado-Valverde J, Mészáros B, Sámano-Sánchez H, Zeke A, Dobson L, Lazar T, Örd M, Nagpal A, et al. (2022). The eukaryotic linear motif resource: 2022 release. Nucleic Acids Res. 50, D497–D508. 10.1093/nar/gkab975. [PubMed: 34718738]

27. Humphreys D, Davidson AC, Hume PJ, Makin LE, and Koronakis V (2013). Arf6 coordinates actin assembly through the WAVE complex, a mechanism usurped by Salmonella to invade

host cells. Proc. Natl. Acad. Sci. USA 110, 16880–16885. 10.1073/pnas.1311680110. [PubMed: 24085844]

28. Kim HR, Gallant C, Leavis PC, Gunst SJ, and Morgan KG (2008). Cytoskeletal remodeling in differentiated vascular smooth muscle is actin isoform dependent and stimulus dependent. Am. J. Physiol. Cell Physiol. 295, C768–C778. 10.1152/ajpcell.00174.2008. [PubMed: 18596213]
29. Maurer-Stroh S, Dickens NJ, Hughes-Davies L, Kouzarides T, Eisenhaber F, and Ponting CP (2003). The tudor domain "royal family": tudor, plant Agenet, chromo, PWWP and MBT domains. Trends Biochem. Sci. 28, 69–74. 10.1016/S0968-0004(03)00004-5. [PubMed: 12575993]
30. Adinolfi S, Bagni C, Musco G, Gibson T, Mazzarella L, and Pastore A (1999). Dissecting FMR1, the protein responsible for fragile X syndrome, in its structural and functional domains. RNA N Y N 5, 1248–1258.
31. Mellacheruvu D, Wright Z, Couzens AL, Lambert JP, St-Denis NA, Li T, Miteva YV, Hauri S, Sardiu ME, Low TY, et al. (2013). The CRAPome: a contaminant repository for affinity purification-mass spectrometry data. Nat. Methods 10, 730–736. 10.1038/nmeth.2557. [PubMed: 23921808]
32. Egile C, Rouiller I, Xu XP, Volkmann N, Li R, and Hanein D (2005). Mechanism of filament nucleation and branch stability revealed by the structure of the Arp2/3 complex at actin branch junctions. PLoS Biol. 3, e383. 10.1371/journal.pbio.0030383. [PubMed: 16262445]
33. Duggirala A, Kimura TE, Sala-Newby GB, Johnson JL, Wu YJ, Newby AC, and Bond M (2015). cAMP-induced actin cytoskeleton remodelling inhibits MKL1-dependent expression of the chemotactic and pro-proliferative factor, CCN1. J. Mol. Cell. Cardiol. 79, 157–168. 10.1016/j.yjmcc.2014.11.012. [PubMed: 25446180]
34. Ngo P, Ramalingam P, Phillips JA, and Furuta GT (2006). Collagen gel contraction assay. Methods Mol. Biol. 341, 103–109. 10.1385/1-59745-113-4:103.
35. Wirth A, Benyó Z, Lukasova M, Leutgeb B, Wettschureck N, Gorbey S, Orsy P, Horváth B, Maser-Gluth C, Greiner E, et al. (2008). G12-G13-LARG-mediated signaling in vascular smooth muscle is required for salt-induced hypertension. Nat. Med. 14, 64–68. 10.1038/nm1666. [PubMed: 18084302]
36. Winograd C, and Ceman S (2011). Fragile X family members have important and non-overlapping functions. Biomol. Concepts 2 (5), 343–352. 10.1515/BMC.2011.033. [PubMed: 25962042]
37. He Q, and Ge W (2017). The tandem Agenet domain of fragile X mental retardation protein interacts with FUS. Sci. Rep. 7, 962. 10.1038/s41598-017-01175-8. [PubMed: 28424484]
38. De Rubeis S, Pasciuto E, Li KW, Fernández E, Di Marino D, Buzzi A, Ostroff LE, Klann E, Zwartkruis FJT, Komiyama NH, et al. (2013). CYFIP1 coordinates mRNA translation and cytoskeleton remodeling to ensure proper dendritic spine formation. Neuron 79, 1169–1182. 10.1016/j.neuron.2013.06.039. [PubMed: 24050404]
39. Schenck A, Bardoni B, Moro A, Bagni C, and Mandel JL (2001). A highly conserved protein family interacting with the fragile X mental retardation protein (FMRP) and displaying selective interactions with FMRP-related proteins FXR1P and FXR2P. Proc. Natl. Acad. Sci. USA 98, 8844–8849. 10.1073/pnas.151231598. [PubMed: 11438699]
40. Darnell JC, Van Driesche SJ, Zhang C, Hung KYS, Mele A, Fraser CE, Stone EF, Chen C, Fak JJ, Chi SW, et al. (2011). FMRP stalls ribosomal translocation on mRNAs linked to synaptic function and autism. Cell 146, 247–261. 10.1016/j.cell.2011.06.013. [PubMed: 21784246]
41. Brown V, Jin P, Ceman S, Darnell JC, O'Donnell WT, Tenenbaum SA, Jin X, Feng Y, Wilkinson KD, Keene JD, et al. (2001). Microarray identification of FMRP-associated brain mRNAs and altered mRNA translational profiles in fragile X syndrome. Cell 107, 477–487. 10.1016/s0092-8674(01)00568-2. [PubMed: 11719188]
42. Castets M, Schaeffer C, Bechara E, Schenck A, Khandjian EW, Luche S, Moine H, Rabilloud T, Mandel JL, and Bardoni B (2005). FMRP interferes with the Rac1 pathway and controls actin cytoskeleton dynamics in murine fibroblasts. Hum. Mol. Genet. 14, 835–844. 10.1093/hmg/ddi077. [PubMed: 15703194]
43. Nolze A, Schneider J, Keil R, Lederer M, Hüttelmaier S, Kessels MM, Qualmann B, and Hatzfeld M (2013). FMRP regulates actin filament organization via the armadillo protein p0071. RNA N Y N 19, 1483–1496. 10.1261/rna.037945.112.

44. Zhang W, Huang Y, and Gunst SJ (2012). The small GTPase RhoA regulates the contraction of smooth muscle tissues by catalyzing the assembly of cytoskeletal signaling complexes at membrane adhesion sites. J. Biol. Chem. 287, 33996–34008. 10.1074/jbc.M112.369603. [PubMed: 22893699]
45. Koronakis V, Hume PJ, Humphreys D, Liu T, Hørning O, Jensen ON, and McGhie EJ (2011). WAVE regulatory complex activation by cooperating GTPases Arf and Rac1. Proc. Natl. Acad. Sci. USA 108, 14449–14454. 10.1073/pnas.1107666108. [PubMed: 21844371]
46. Tang DD, and Anfinogenova Y (2008). Physiologic properties and regulation of the actin cytoskeleton in vascular smooth muscle. J. Cardiovasc. Pharmacol. Therapeut. 13, 130–140. 10.1177/1074248407313737.
47. Guilluy C, Brégeon J, Toumaniantz G, Rolli-Derkinderen M, Retailleau K, Loufrani L, Henrion D, Scalbert E, Bril A, Torres RM, et al. (2010). The Rho exchange factor Arhgef1 mediates the effects of angiotensin II on vascular tone and blood pressure. Nat. Med. 16, 183–190. 10.1038/nm.2079. [PubMed: 20098430]
48. Zhang W, Bhetwal BP, and Gunst SJ (2018). Rho kinase collaborates with p21-activated kinase to regulate actin polymerization and contraction in airway smooth muscle. J. Physiol. 596, 3617–3635. 10.1113/JP275751. [PubMed: 29746010]
49. Gabunia K, Herman AB, Ray M, Kelemen SE, England RN, DeLa Cadena R, Foster WJ, Elliott KJ, Eguchi S, and Autieri MV (2017). Induction of MiR133a expression by IL-19 targets LDLRAP1 and reduces oxLDL uptake in VSMC. J. Mol. Cell. Cardiol. 105, 38–48. 10.1016/j.yjmcc.2017.02.005. [PubMed: 28257760]
50. Cooper HA, Cicalese S, Preston KJ, Kawai T, Okuno K, Choi ET, Kasahara S, Uchida HA, Otaka N, Scalia R, et al. (2021). Targeting mitochondrial fission as a potential therapeutic for abdominal aortic aneurysm. Cardiovasc. Res. 117, 971–982. 10.1093/cvr/cvaa133. [PubMed: 32384150]
51. Haines DS, Lee JE, Beauparlant SL, Kyle DB, den Besten W, Sweredoski MJ, Graham RLJ, Hess S, and Deshaies RJ (2012). Protein interaction profiling of the p97 adaptor UBXD1 points to a role for the complex in modulating ERGIC-53 trafficking. Mol. Cell. Proteomics 11, M111.016444. 10.1074/mcp.M111.016444.
52. Cox J, and Mann M (2008). MaxQuant enables high peptide identification rates, individualized p.p.b.-range mass accuracies and proteome-wide protein quantification. Nat. Biotechnol. 26, 1367–1372. 10.1038/nbt.1511. [PubMed: 19029910]
53. Cox J, Neuhauser N, Michalski A, Scheltema RA, Olsen JV, and Mann M (2011). Andromeda: a peptide search engine integrated into the MaxQuant environment. J. Proteome Res. 10, 1794–1805. 10.1021/pr101065j. [PubMed: 21254760]
54. Vrakas CN, Herman AB, Ray M, Kelemen SE, Scalia R, and Autieri MV (2019). RNA stability protein ILF3 mediates cytokine-induced angiogenesis. FASEB J Off Publ Fed Am Soc Exp Biol 33, 3304–3316. 10.1096/fj.201801315R.
55. Herman AB, Silva Afonso M, Kelemen SE, Ray M, Vrakas CN, Burke AC, Scalia RG, Moore K, and Autieri MV (2019). Regulation of stress granule formation by inflammation, vascular injury, and atherosclerosis. Arterioscler. Thromb. Vasc. Biol. 39, 2014–2027. 10.1161/ATVBAHA.119.313034. [PubMed: 31462091]
56. Cuneo AA, Herrick D, and Autieri MV (2010). Il-19 reduces VSMC activation by regulation of mRNA regulatory factor HuR and reduction of mRNA stability. J. Mol. Cell. Cardiol. 49, 647–654. 10.1016/j.yjmcc.2010.04.016. [PubMed: 20451530]
57. Gabunia K, Ellison S, Kelemen S, Kako F, Cornwell WD, Rogers TJ, Datta PK, Ouimet M, Moore KJ, and Autieri MV (2016). IL-19 halts progression of atherosclerotic plaque, polarizes, and increases cholesterol uptake and efflux in macrophages. Am. J. Pathol. 186, 1361–1374. 10.1016/j.ajpath.2015.12.023. [PubMed: 26952642]
58. Ray M, Gabunia K, Vrakas CN, Herman AB, Kako F, Kelemen SE, Grisanti LA, and Autieri MV (2018). Genetic deletion of IL-19 (Interleukin-19) exacerbates atherogenesis in Il19−/−×Ldlr−/− double knockout mice by dysregulation of mRNA stability protein HuR (human antigen R). Arterioscler. Thromb. Vasc. Biol. 38, 1297–1308. 10.1161/ATVBAHA.118.310929. [PubMed: 29674474]
59. Gabunia K, Jain S, England RN, and Autieri MV (2011). Anti-inflammatory cytokine interleukin-19 inhibits smooth muscle cell migration and activation of cytoskeletal regulators

of VSMC motility. Am. J. Physiol. Cell Physiol. 300, C896–C906. 10.1152/ajpcell.00439.2010. [PubMed: 21209363]

Highlights

- FXR1 interacts with cytoskeletal RNAs to regulate their abundance and stability
- FXR1 interacts with cytoskeletal proteins, such as WAVE proteins CYFIP1 and ARP2
- FXR1 regulates cytoskeletal-dependent processes in vascular smooth muscle cells
- The genetic deletion of FXR1 in smooth muscle decreases blood pressure in mice

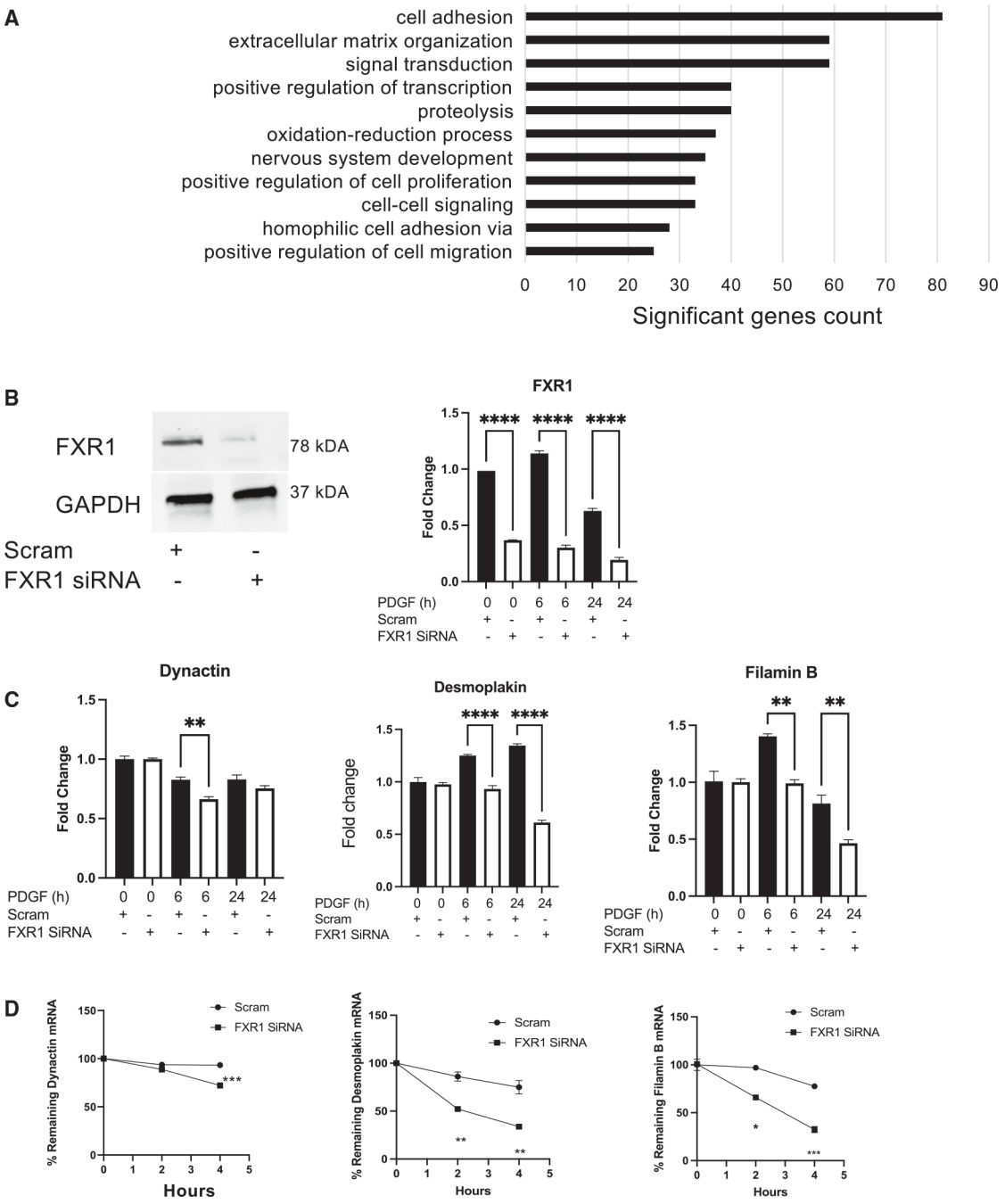

Figure 1. RNA immunoprecipitation sequencing and effects of FXR1 deletion on cytoskeletal mRNA stability

(A) Gene Ontology analysis of mRNA transcripts identified by RNA immunoprecipitation sequencing (RIP-seq). Primary human VSMCs were transduced with FLAG-tagged AdFXR1 and immunoprecipitated with anti-FLAG antibody, and interacting transcripts were identified by RIP-seq.

(B) qRT-PCR and representative western blot validating FXR1 knockdown with specific siRNA.

(C) Depletion of FXR1 significantly reduces cytoskeletal mRNA abundance of selected cytoskeletal-associated transcripts.
(D) Deletion of FXR1 results in reduced mRNA stability of selected cytoskeletal-associated transcripts.
To determine mRNA stability, samples were stimulated with PDGF-AB for 16 h, actinomycin D added, RNA isolated at the indicated time points, and mRNA quantified by RT-PCR.
*$p < 0.05$, **$p < 0.01$, ***$p < 0.001$, and ****$p < 0.0001$ from at least three experiments.

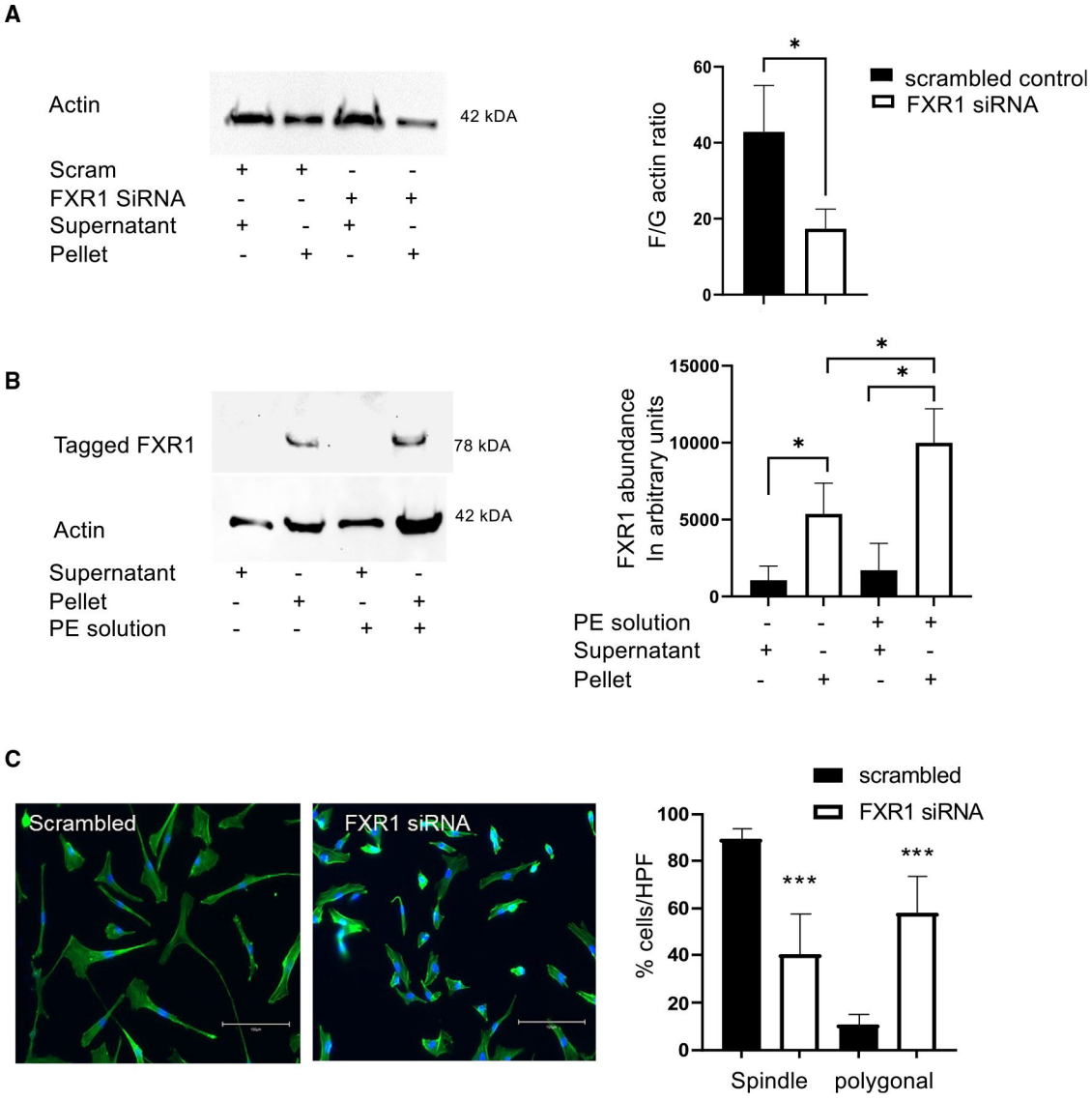

Figure 2. FXR1 regulates actin dynamics

(A) FXR1 regulates actin polymerization. Human VSMCs (hVSMCs) transfected with FXR1 siRNA or scrambled control were lysed in actin stabilization buffer followed by centrifugation to separate the F-actin from G-actin pool. Lysates were separated by SDS-PAGE and actin detected by western blot and quantified by ImageJ. The ratio of F-actin to G-actin was lower in hVSMCs in which FXR1 was depleted by siRNA compared with controls quantified from densitometry from three independent experiments.

(B) FXR1 preferentially co-sediments with F-actin. hVSMCs transduced with FLAG-tagged AdFXR1 were lysed in actin stabilization buffer. Addition of polymerization-enhancing (PE) solution, 100× phalloidin, enhances actin polymerization, and significantly more FXR1 co-sediments with F-actin in phalloidin-treated samples compared with untreated samples.

(C) hVSMCs depleted of FXR1 have an altered morphology, with significantly less VSMCs displaying the typical spindle shape indicative of primary cultured hVSMCs and significantly more VSMCs with a polygonal shape. Cells were stained with phalloidin,

counterstained with DAPI, and counted from 4 high-powered fields (hpf) from three independent experiments.

*$p < 0.05$ and ***$p < 0.001$ from at least three experiments.

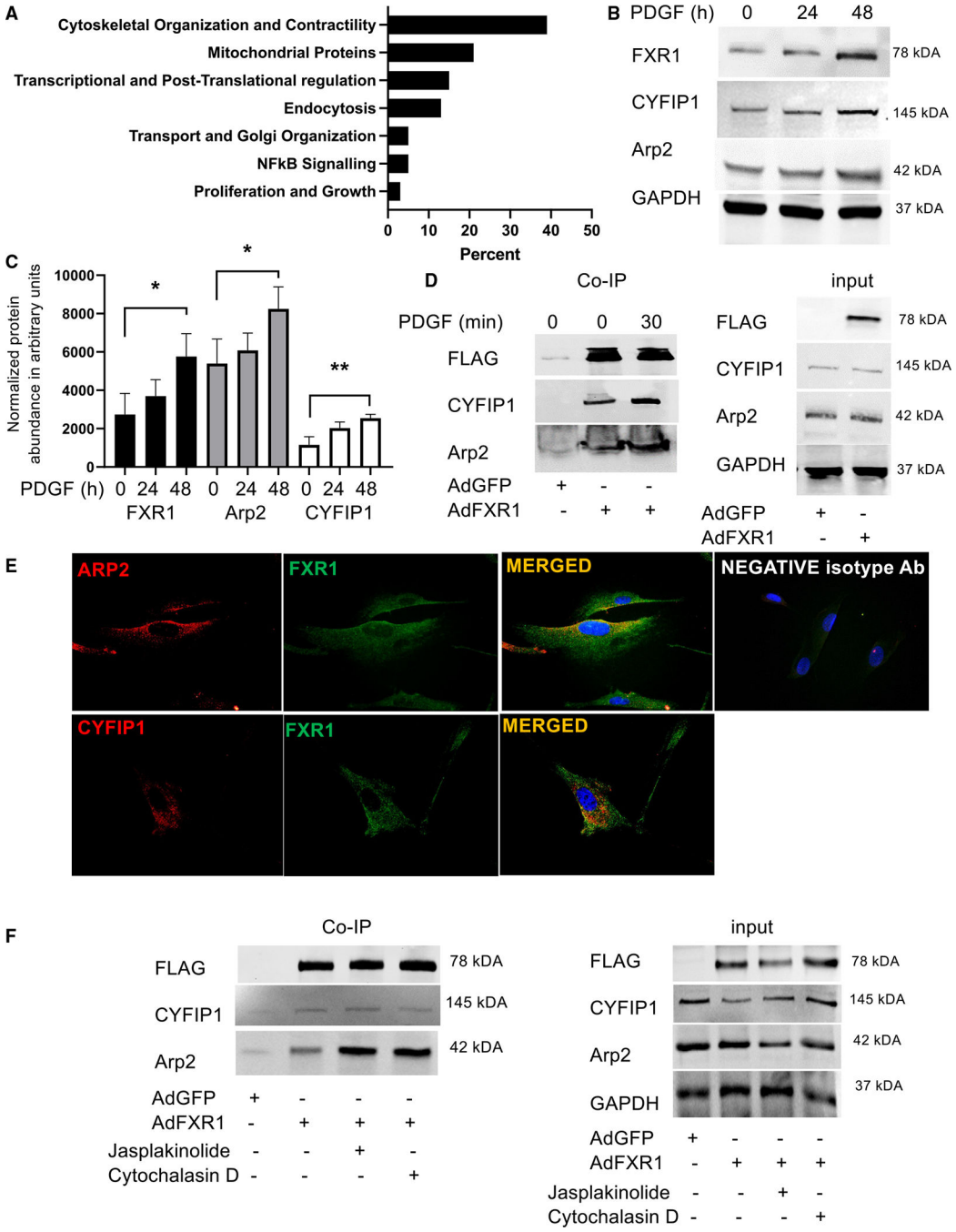

Figure 3. FXR1 interacts with cytoskeletal and WRC proteins

(A) Gene Ontology analysis of proteins immunoprecipitated with FXR1 and identified by mass spectrometry (MS). hVSMCs were transduced with FLAG-tagged AdFXR1 and immunoprecipitated with anti-FLAG antibody, and immunoprecipitated proteins were identified by MS.

(B) FXR1, CYFIP1, and Arp2 are PDGF-responsive proteins in hVSMCs. Representative western blot showing that FXR1, CYFIP1, and Arp2 expression is increased in PDGF-

stimulated hVSMCs. hVSMCs were serum starved for 24 h and then stimulated for the indicated times with PDGF-AB.

(C) Densiometric analysis of increased WAVE protein expression in PDGF-stimulated hVSMCs. FXR2 protein abundance is not increased in response to cytoskeleton-rearranging stimuli (Figure S3).

(D) Validation of protein-protein interactions of CYFIP1 and Arp2 with FXR1. hVSMCs were transduced with AdFXR1 or AdGFP, and FXR1 was immunoprecipitated with anti-FLAG antibody. Some samples were stimulated with PDGF for 30 min. Immunoprecipitated proteins were then identified by western blot using antibody to the shown proteins. Blot shown is representative of at least 3 independent experiments performed.

(E) *In vivo* co-localization of endogenous FXR1 and WAVE proteins. Immunocytochemistry of PDGF-stimulated (30 min) hVSMCs co-stained with antibody specific for FXR1, Arp2, and CYFIP1. FXR1 co-localized with these proteins primarily in the cytoplasm, magnification 600×. Negative isotype control is the same secondary antibody used for each primary antibody, merged.

(F) FXR1 actin dynamics modulate FXR1 protein-protein interactions. hVSMCs were treated with the actin stabilizer jasplakinolide and the actin destabilizer cytochalasin-B prior to co-immunoprecipitation.

*$p < 0.05$ and **$p < 0.01$ from at least three experiments.

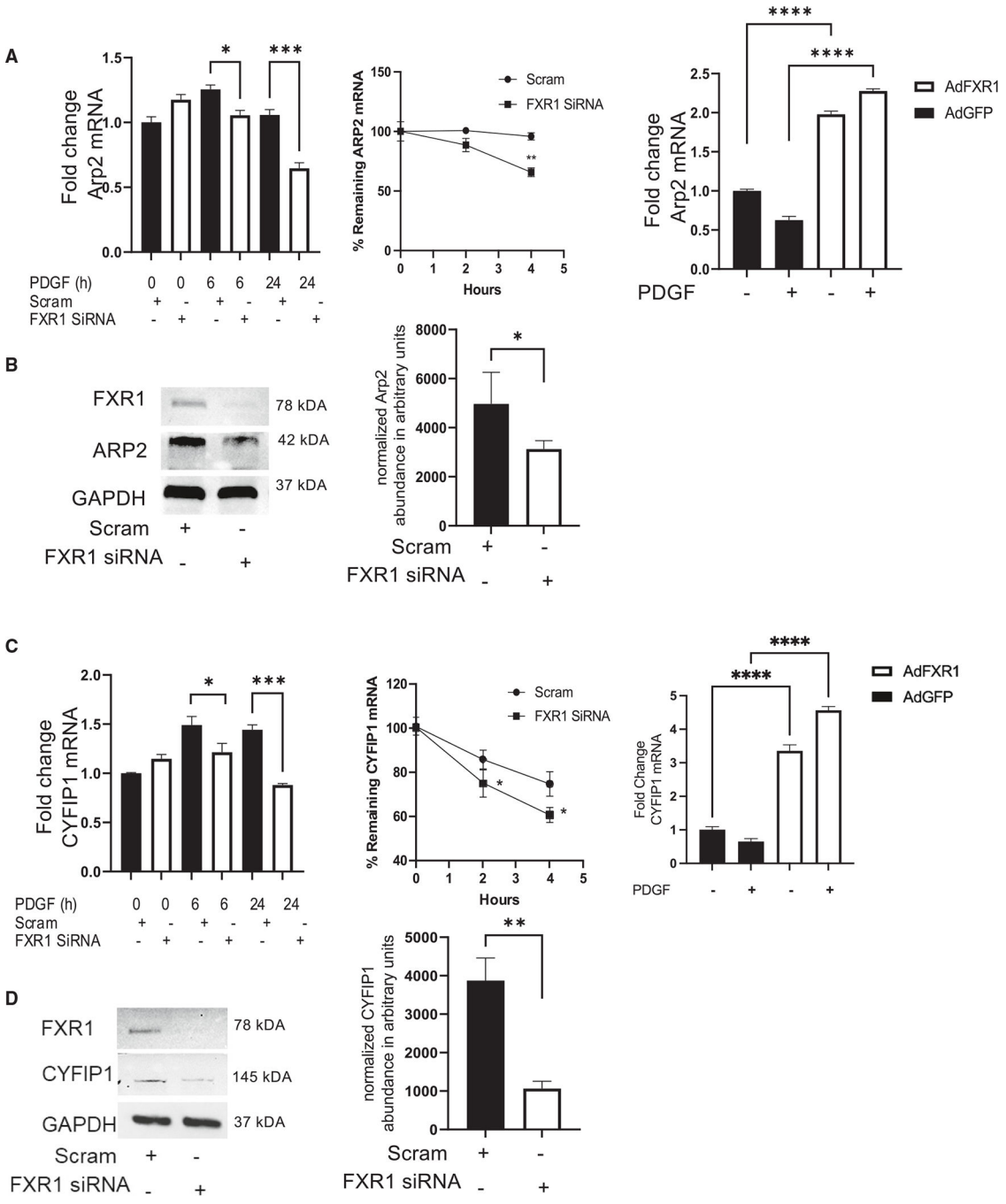

Figure 4. FXR1 knockdown reduces WAVE mRNA abundance, mRNA stability, and protein abundance

hVSMCs were transfected with control or FXR1 siRNA, stimulated with PDGF-AB for the times noted, and total mRNA determined by qRT-PCR. To determine mRNA stability, samples were stimulated with PDGF-AB for 16 h, actinomycin D added, RNA isolated at the indicated time points, and mRNA quantified by RT-PCR. For RIP-PCR, transcripts were recognized and pulled down by FLAG-tagged FXR1 adenovirus, reverse transcribed, and amplified by PCR. For protein abundance, protein was isolated from lysates from hVSMCs

transfected with control or FXR1 siRNA and detected by western blot. Densiometric analysis was determined from 3–5 independent experiments.

(A) Arp2 RNA abundance, stability, and mRNA interaction by RIP-PCR.

(B) Arp2 protein abundance.

(C) CYFIP1 RNA abundance, stability, and mRNA interaction by RIP-PCR.

(D) CYFIP1 protein abundance. Representative blots are shown of at least 3 independent experiments performed.

*$p < 0.05$, **$p < 0.01$, ***$p < 0.001$, and ****$p < 0.0001$ from at least three experiments.

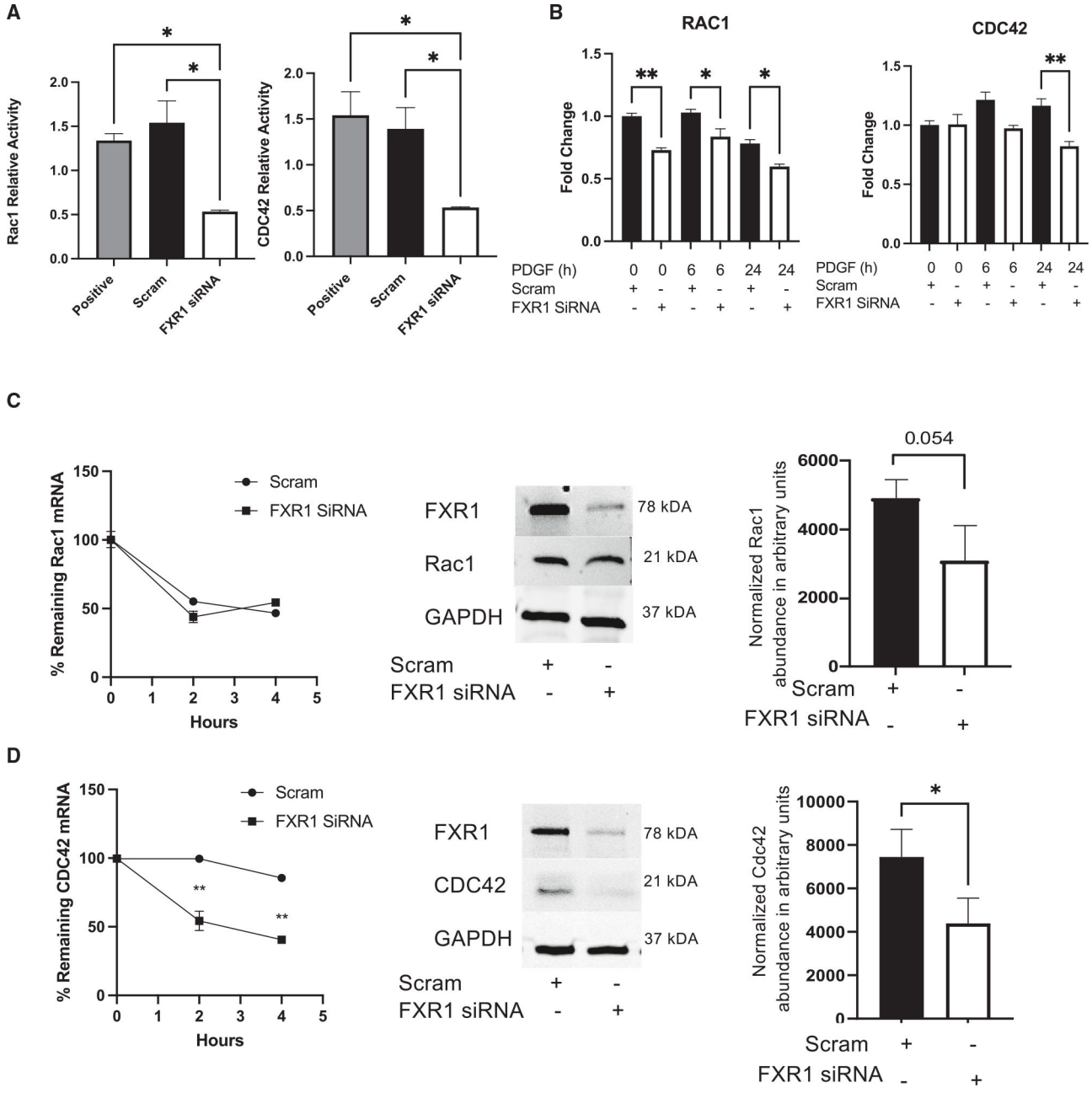

Figure 5. FXR1 depletion reduces GTPase activity

(A) siRNA depletion of FXR1 reduces Rac1 and CDC42 activity in PDGF-stimulated hVSMCs compared with controls. GTPase activity levels were measured by ELISA using a commercially available kit described in the STAR Methods.

(B) siRNA depletion of FXR1 reduces Rac1 and CDC42 mRNA abundance in PDGF-stimulated hVSMCs compared with controls. Cultured hVSMCs were serum reduced for 24 h and then stimulated with 20 ng/mL PDGF-AB for the times indicated.

(C) FXR1 depletion reduces Rac1 protein abundance. Cultured hVSMCs were serum reduced for 24 h and then stimulated with 20 ng/mL PDGF-AB for 24 h. Proteins were identified with specific antibody by chemiluminescence.

(D) FXR1 reduces CDC42 mRNA stability and protein abundance. Cultured hVSMCs were treated as described in (C). Western blot shown is representative of at least three experiments.

*$p < 0.05$, **$p < 0.01$, and ***$p < 0.001$ from at least three experiments.

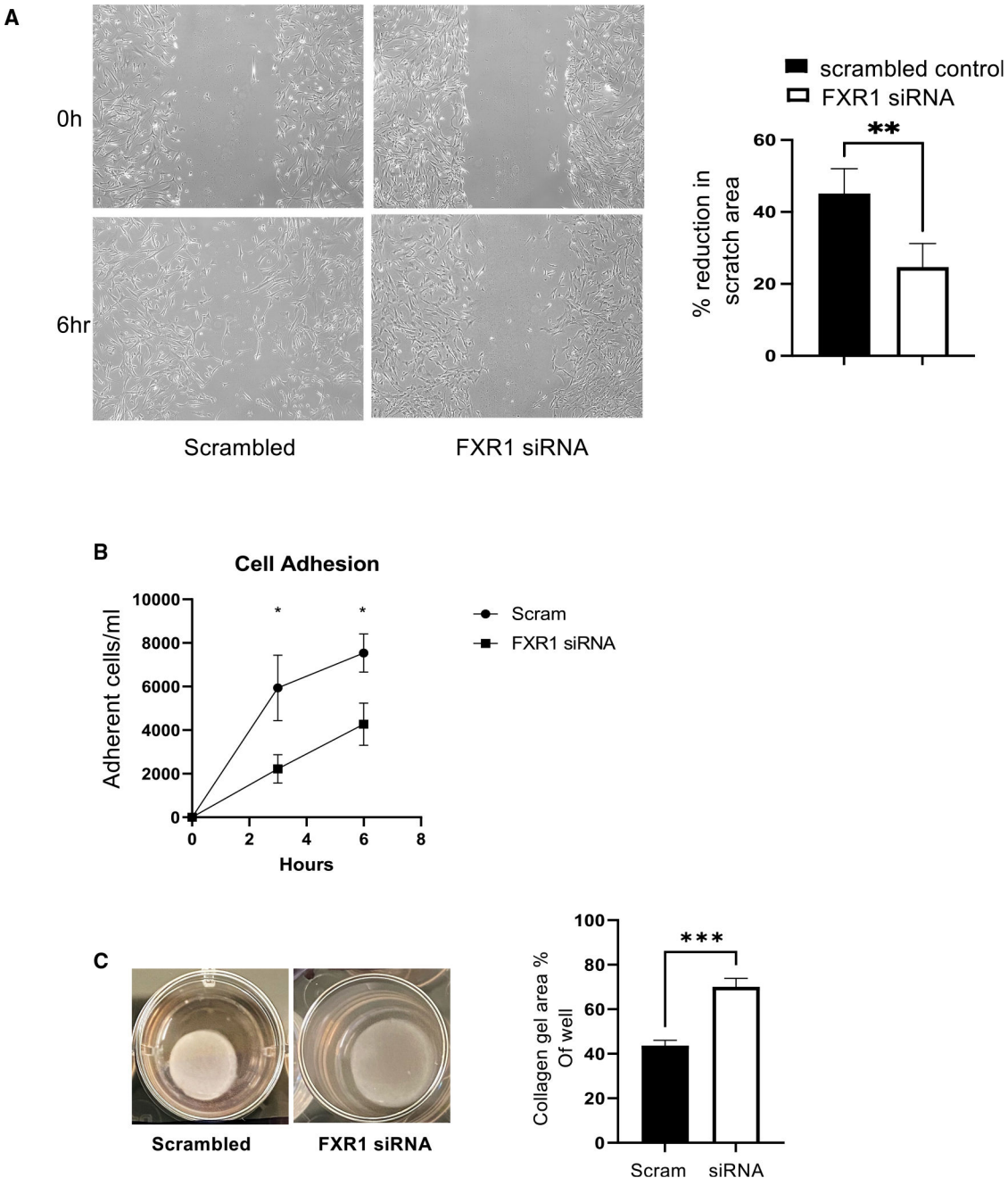

Figure 6. FXR1 knockdown reduces cytoskeletal-dependent processes in hVSMCs

(A) FXR1 knockdown decreases hVSMC migration. hVSMCs were transfected with FXR1 siRNA and scrambled control and seeded on a glass chamber slide. Seventy-two hours post-transfection, images were captured at 6 h after a 2-mm scratch was made. The area of the scratch wound was quantified using ImageJ image analysis from three independent experiments.

(B) FXR1 depletion reduces hVSMC adhesion. Equal numbers of hVSMCs were plated into a 24-well tray 72 h after transfection with FXR1 siRNA or scrambled control. Cells adhered to the plate were counted at 3 and 6 h.

(C) FXR1 siRNA knockdown inhibits hVSMC contraction. hVSMCs were suspended into collagen gels as described in STAR Methods. Collagen gels were photographed after 72 h, and gel surface area was calculated by ImageJ in triplicate.
**$p < 0.001$.

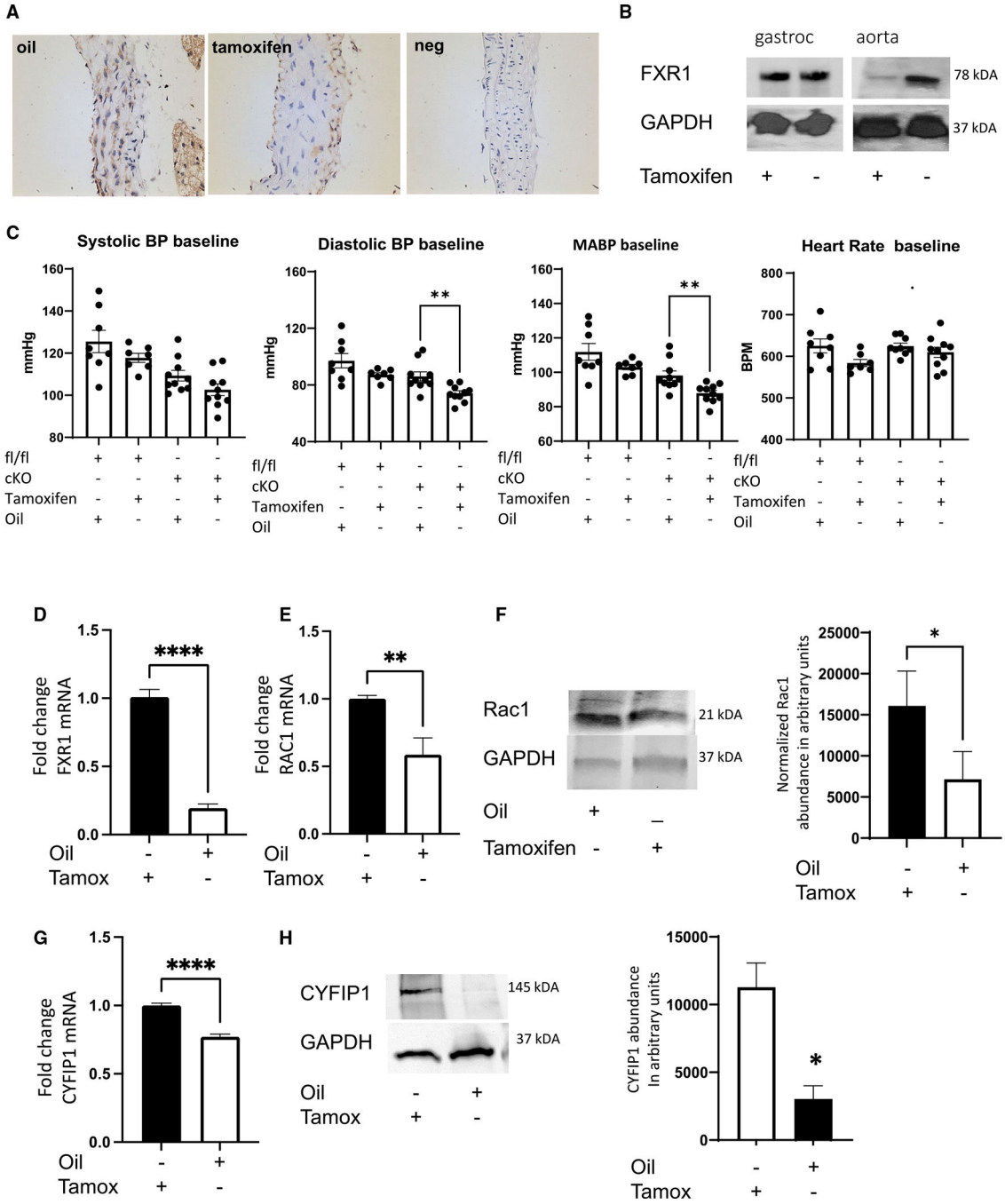

Figure 7. Conditional SMC-specific FXR1 knockout mice are hypotensive

(A) Conditional expression of FXR1. Immunohistochemistry of FXR1 protein in conditional $FXR1^{SMC/SMC}$ mice following 5 days of intraperitoneal (i.p.) tamoxifen injections (80 μg/kg/day) or corn oil. Figure shows FXR1 expression (red-brown staining) only in endothelium and adventitia of tamoxifen-injected mice.

(B) Western blot from gastroc and aorta showing differing FXR1 expression following tamoxifen injections.

(C) Conditional FXR1$^{smc/smc}$ mice have decreased diastolic and mean arterial blood pressure compared with controls. Telemetric measurements were taken for 26 h. **$p < 0.001$. WRC, GTPase, and cytoskeleton-associated gene expression are reduced in aorta from FXR1$^{SMC/SMC}$.

(D) RNA isolated from aorta from mice injected with oil or tamoxifen were subjected to qRT-PCR to validate FXR1 knockout.

(E and F) Rac1 mRNA and protein are significantly decreased in aorta from tamoxifen-injected compared with control mice.

(G and H) CYFIP1 mRNA and protein are significantly decreased in aorta from tamoxifen-injected compared with control mice. Western blot shown is representative of at least 3 experiments performed from aorta from at least 3 mice.

*$p < 0.05$, **$p < 0.01$, and ***$p < 0.001$ from at least three aortas.

KEY RESOURCES TABLE

REAGENT or RESOURCE	SOURCE	IDENTIFIER
Antibodies		
Rabbit monoclonal anti – FXR1	Cell Signaling	Cat #12295; RRID: AB_2797875
Rabbit monoclonal anti – CYFIP1	Cell Signaling	Cat #81221
Rabbit monoclonal anti – ARP2	Proteintech	Cat #10922 1-AP; RRID: AB_2221854
Rabbit monoclonal anti – FLAG	Proteintech	Cat #20543-I-AP; RRID: AB_11232216
Rabbit monoclonal anti – GAPDH	Cell Signaling	Cat #2118; RRID: AB_561053
Rabbit polyclonal anti – CDC42	Proteintech	Cat #10155–1-AP; RRID: AB_2078096
Mouse monoclonal anti – RAC1	Abcam	Cat #33186–125; RRID: AB_777598
Rabbit polyclonal anti – FXR2	GeneTex	Cat #GTX109465; RRID: AB_11176053
Anti – FLAG M2 Affinity Beads	Sigma Aldrich	Cat #A2220; RRID: AB_10063035
Bacterial and virus strains		
Adeno-FXRI	Vector Biolabs	Cat #ADV-209437
Adeno- GFP	Vector Biolabs	Cat #1060
Chemicals, peptides, and recombinant proteins		
Recombinant Human PDGF – AB	Peprotech	Cat #100–00AB
Jasplakinolide	Cayman Chemicals	Cat #102396–24-7
Cytochalasin D	Sigma Aldrich	Cat #22144–77-0
Tamoxifen	Cayman Chemicals	Cat #13258
Rat Tail Type I Collagen Solution	Advanced BiomatiX	Cat #5153
Actinomycin D	Cayman Chemicals	Cat #11421
Critical commercial assays		
RT2 Profiler™ PCR Array Mouse Cytoskeleton Regulators	Qiagen	Cat# PAMM-049Z
Actin Polymerization Kit	Cytoskeleton, Inc	Cat# BK037
CDC42 G-LISA Activation Kit	Cytoskeleton, Inc	Cat #BK127
Rac1 G-LISA Activation Kit	Cytoskeleton, Inc	Cat #BK128
Deposited data		
RNA-Immunoprecipitation Seq	This paper	N/A
Mass spectrometry	This paper	N/A
Experimental models: Cell lines		
Human Primary VSMC	Lonza Corporation	Cat #CC-2571
Experimental models: Organisms/strains		
Mouse: FXR1 F/F	Fragile X Research Foundation	fraxa.org/fragile-x0research/resources

REAGENT or RESOURCE	SOURCE	IDENTIFIER
Mouse: SmMHC-CreER^{T2}	Jackson Labs	https://www.jax.org/strain/019079; RRID: IMSR_JAX:019079
Mouse: FXR1$^{vsm/vsm}$	This paper	N/A
Oligonucleotides		
ON-TARGETplus Human FXR1 siRNA	Dharmacon, Inc	Cat #0121011–00-0010
ON-TARGETplus Non-targeting Control siRNA (Scram)	Dharmacon, Inc	Cat #001810–01-05
Primers for XX see STAR Methods	Integrated DNA technologies	N/A
Software and algorithms		
ImageJ	This paper	https://imagej.nih.gov/ij/
Graph Pad Prism Version 8	Dotmatrics	https://www.graphpad.com